Universität Karlsruhe (TH)
Institut für Baustatik

Theory and Numerics of Three–Dimensional Beams with Elastoplastic Material Behaviour

F. Gruttmann, R. Sauer, W. Wagner

Mitteilung 1(1999)

Universität Karlsruhe (TH)
Institut für Baustatik

Theory and Numerics of Three–Dimensional Beams with Elastoplastic Material Behaviour

F. Gruttmann, R. Sauer, W. Wagner

Mitteilung 1(1999)

Prof. Dr.–Ing. W. Wagner
Institut für Baustatik
Universität Karlsruhe
Postfach 6980
76128 Karlsruhe

Telefon: (0721) 608–2280
Telefax: (0721) 608–6015
E–mail: bs@.uni-karlsruhe.de
Internet: http://www.bs.uni-karlsruhe.de

©

THEORY AND NUMERICS OF THREE–DIMENSIONAL BEAMS WITH ELASTOPLASTIC MATERIAL BEHAVIOUR *

F. Gruttmann[1], R. Sauer[2], W. Wagner[3]

[1] *Institut für Statik, Technische Universität Darmstadt, 64283 Darmstadt, Germany* ,
[2] *Ingenieurbüro Jäger, 01445 Radebeul, Germany*,
[3] *Institut für Baustatik, Universität Karlsruhe, 76128 Karlsruhe, Germany*

Keywords:
Three-dimensional beams, finite deformations, torsion warping deformation, arbitrary cross sections, elastoplastic material behaviour, finite elements

ABSTRACT

A theory of space curved beams with arbitrary cross–sections and an associated finite element formulation is presented. Within the present beam theory the reference point, the centroid, the center of shear and the loading point are arbitrary points of the cross–section. The beam strains are based on a kinematic assumption where torsion–warping deformation is included. Each node of the derived finite element possesses seven degrees of freedom. The update of the rotational parameters at the finite element nodes is achieved in an additive way. Applying the isoparametric concept the kinematic quantities are approximated using Lagrangian interpolation functions. Since the reference curve lies arbitrarily with respect to the centroid the developed element can be used to discretize eccentric stiffener of shells. Due to the implemented constitutive equations for elastoplastic material behaviour the element can be used to evaluate the load carrying capacity of beam structures.

1 INTRODUCTION

Three–dimensional beam–like structures undergoing finite deformations occur in different areas of engineering practice. Here motions of flexible beams like helicopter blades, rotor blades, robot arms or beams in space–structure technology are mentioned. Furthermore, the analysis of load carrying capacities requires the implementation of constitutive equations for inelastic material behaviour. Numerous papers have been published up to now using different approaches. Some of them are discussed in the following.
Due to the non–commutativity of successive finite rotations about fixed axes, Argyris et al.[1] introduced the so–called semi–tangential rotations to circumvent this difficulty. Bathe and Bolourchi [2] developed an updated and a total Lagrangian formulation for beams with large displacements. Thin structures undergoing finite deformations are usually characterized by significant rigid body motions. This motivates the so–called

*dedicated to F.G. Kollmann on the occasion of his 65th birthday

co–rotational formulation where the rigid body motions are separated from the total deformation (e.g. see Belytschko and Hsieh [3], Crisfield [4] or Nour–Omid [5]). Applying this procedure existing linear elements can be used for nonlinear computations.
Several authors developed finite element formulations for three–dimensional beams using beam strains derived from the internal virtual work, see Reissner [6]. Here we mention the papers of Simo and Vu–Quoc [7, 8] and Cardona and Géradin [9]. The authors in [7] show that the linearization of the virtual work principle yields a non–symmetric geometric tangent stiffness matrix when applying a multiplicative update of the rotation tensor. The tangent matrix is only symmetric at a point of equilibrium assuming conservative loads. Ibrahimbegović [10] derived symmetric tangent matrices when using an additive update of the axial vector.
Most of the finite element formulations are concerned with beams where centroid and center of shear coincide. The problem of coupled bending torsion deformation of beams has been studied theoretically e.g. by Reissner [11, 12]. In Ref. [8] torsion–warping deformation has been incorporated within the theory and the associated finite element formulation.

In this paper we derive a three–dimensional finite beam–element with arbitrary space curved reference axis. The novel aspects and essential features of the formulation are summarized as follows:

(i) The introduced beam strains based on a kinematic assumption including torsion–warping deformation are conform with the strains in Ref. [8]. Here, we additionally derive the relation to the Green–Lagrangian strains and the associated variations. In our formulation the matrix which relates the variation of the Green–Lagrangian strains to the variational beam strains depends on the deformation. Thus the complete nonlinearity within the underlying kinematic assumption is considered in the present theory. Due to this fact the numerical results show a good agreement with the results of higher valued models like shell discretizations for thin–walled structures.

(ii) The constitutive equations for elastoplastic material behaviour are implemented. Within the present beam theory the normal stress and the shear stresses enter into the von Mises yield condition and the associated flow rule. Thus interaction between the different stress components is included. The nonlinear stress–strain relations requires a numerical integration over the cross–sections. The developed element can be used to analyze the carrying capacity of beam structures.

(iii) For linear elasticity and small strains the material matrix can be integrated analytically. For this purpose one has to apply the equations of Saint–Venant torsion theory along with Green's formula to integrate the so–called warping coordinates. This yields a material matrix in terms of section quantities which describes the coupling effects. In contrast to Ref. [8] the reference point is an arbitrary point of the cross–section.

(iv) The finite element formulation is presented using Lagrangian interpolation functions. Each node possesses seven degrees of freedom at the nodes. The update of the nodal rotation quantities is performed in an additive way. Within this procedure additional storage of the rotation matrix with nine parameters can be avoided. The

linearization yields a symmetric tangent matrix. However, due to the chosen finite element approximation the expressions are essentially simpler compared with Ref. [10]. The external loading can be applied at an arbitrary point of the cross–section. The contribution of the loads to the stiffness matrix is derived. Loading with stress couple resultants leads to a symmetric load stiffness matrix. This is in contrast to the multiplicative procedure, see Ref. [7].

The contents of the paper is outlined as follows:
In the next section we present the kinematics of a space curved beam. The beam strains are defined and the relation to the Green–Lagrangian strains is shown. In section 3 the underlying variational formulation of the boundary value problem is given using a Lagrangian representation. The associated Euler–Lagrange equations are derived. Furthermore the linearized variational formulation is described. In section 4 the basic equations for elastoplastic material behaviour are given. For linear elasticity and small strains the material matrix which describes the torsion bending coupling is derived in terms of section quantities. The associated finite element formulation is given in section 5. The applicability of the developed formulation is demonstrated in section 6 with several examples. Comparisons with results obtained with shell discretizations are given.

2 KINEMATIC DESCRIPTION OF THE BEAM

A beam with reference configuration denoted by $\mathcal{B}_0$ according to Fig. 1 is considered. Assuming arbitrary cross–sections the centroid S and the center of shear M are independent of the reference point O. An orthogonal basis system $\mathbf{A}_i$ with local coordinates $\{\xi_1, \xi_2, \xi_3\}$ is introduced. The axis of the beam is initially along $\mathbf{A}_1$ with the arc–length parameter $S = \xi_1 \in [0, L]$ of the spatial curve. The cross–sections of the beam therefore lie in planes described by the basis vectors $\{\mathbf{A}_2, \mathbf{A}_3\}$. Accordingly the frame $\mathbf{a}_i$ is defined in the current configuration which is characterized by the time parameter t. Note, that within the underlying beam kinematic the vector $\mathbf{a}_1$ is not tangent vector of the deformed reference curve.
The basis vectors $\mathbf{A}_i$ and $\mathbf{a}_i$ follow from the orthogonal transformations

$$\mathbf{A}_i(S) = \mathbf{R}_0(S)\,\mathbf{e}_i\,, \qquad \mathbf{a}_i(S,t) = \mathbf{R}(S,t)\,\mathbf{e}_i \qquad \text{with} \qquad \mathbf{R}_0, \mathbf{R} \in SO(3)\,. \tag{1}$$

Several parametrizations of orthogonal tensor using Eulerian angles, Cardan angles, quaternions etc. have been discussed in the literature, see e.g. Géradin and Rixen [13], Betsch et al. [14].
The position vectors of the undeformed and deformed cross–sections are given with the following kinematic assumption

$$\begin{aligned} \mathbf{X}(\xi_2, \xi_3, S) &= \mathbf{X}_0(S) + \xi_2 \mathbf{A}_2(S) + \xi_3 \mathbf{A}_3(S) \\ \mathbf{x}(\xi_2, \xi_3, S, t) &= \mathbf{x}_0(S,t) + \xi_2 \mathbf{a}_2(S,t) + \xi_3 \mathbf{a}_3(S,t) + \alpha(S,t)\,\bar{w}(\xi_2, \xi_3)\,\mathbf{a}_1(t) \end{aligned} \tag{2}$$

where $\mathbf{a}_1$ is assumed to be piecewise constant. The given warping function $\bar{w}(\xi_2, \xi_3)$ is defined within the Saint–Venant torsion theory for bars. This is a basic assumption which restricts the present formulation to a certain class of problems. Our numerical investigations however showed good agreement of the results for thin–walled beam structures obtained with the present beam model compared with a higher valued shell model.

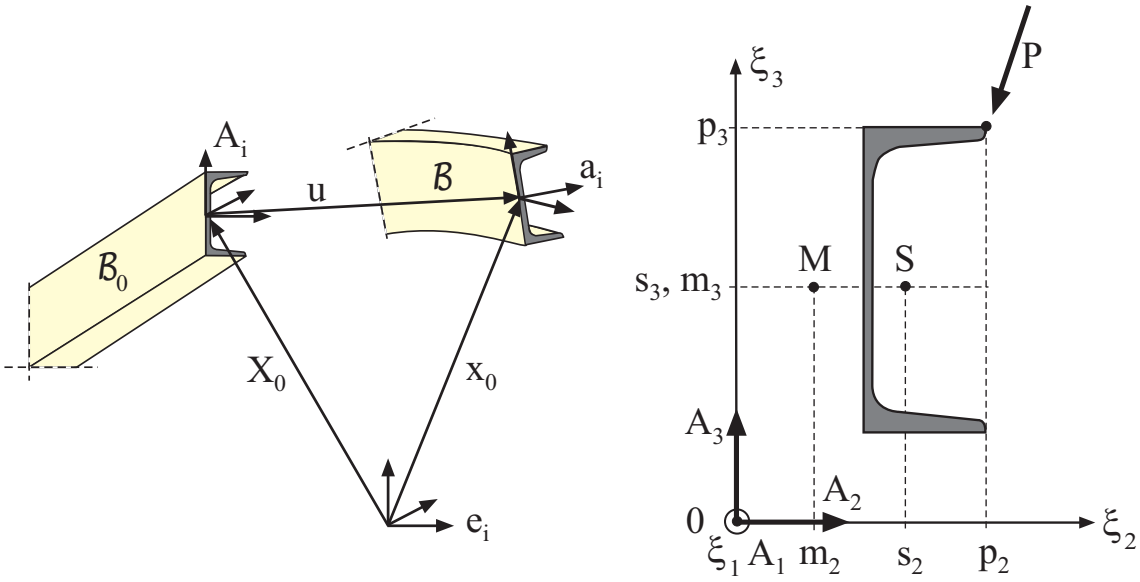

Figure 1: Initial and current configuration of the beam

For linear elasticity and pure torsion the boundary value problem is given with the following Neumann problem, see e.g. Timoshenko and Goodier [15]

$$\begin{aligned} \bar{w}_{,22} + \bar{w}_{,33} &= 0 && \text{in} \quad A \\ \bar{w}_{,2}\, n_2 + \bar{w}_{,3}\, n_3 &= \xi_3\, n_2 - \xi_2 n_3 && \text{on} \quad C\,, \end{aligned} \tag{3}$$

where the outward normal vector $\mathbf{n} = [n_2, n_3]^T$ is defined on the boundary C. Here, the notation $(\cdot)_{,\beta}$ is used to denote partial derivatives with respect to the coordinates ξ_β. The solution of (3) along with the normality conditions

$$\int_A \tilde{w}\, dA = 0\,, \qquad \int_A \tilde{w}\, \xi_2\, dA = 0\,, \qquad \int_A \tilde{w}\, \xi_3\, dA = 0 \tag{4}$$

define the center of shear M with coordinates $\{m_2, m_3\}$. The warping function $\tilde{w}$ refers to M and reads

$$\tilde{w} = \bar{w} + m_2 \bar{\xi}_3 - m_3 \bar{\xi}_2 \tag{5}$$

where the coordinates $\bar{\xi}_2 = \xi_2 - s_2$ and $\bar{\xi}_3 = \xi_3 - s_3$ intersect at the centroid S.
Based on the kinematic assumption (2) the tangent vectors $\mathbf{G}_i = \mathbf{X}_{,i}$ and $\mathbf{g}_i = \mathbf{x}_{,i}$ are derived

$$\begin{aligned} \mathbf{G}_1 &= \mathbf{X}_0' + \xi_2 \mathbf{A}_2' + \xi_3 \mathbf{A}_3' & \mathbf{g}_1 &= \mathbf{x}_0' + \xi_2 \mathbf{a}_2' + \xi_3 \mathbf{a}_3' + \alpha'\, \bar{w} \mathbf{a}_1 \\ \mathbf{G}_2 &= \mathbf{A}_2 & \mathbf{g}_2 &= \mathbf{a}_2 + \alpha\, \bar{w}_{,2}\, \mathbf{a}_1 \\ \mathbf{G}_3 &= \mathbf{A}_3 & \mathbf{g}_3 &= \mathbf{a}_3 + \alpha\, \bar{w}_{,3}\, \mathbf{a}_1 \end{aligned} \tag{6}$$

where $(\cdot)'$ denotes the customary symbol for differentiation with respect to the arc–length. The derivative of the orthogonal basis systems can be expressed using the vector products $\mathbf{A}_i' = \boldsymbol{\theta}_0 \times \mathbf{A}_i$ and $\mathbf{a}_i' = \boldsymbol{\theta} \times \mathbf{a}_i$, where $\boldsymbol{\theta}_0$ and $\boldsymbol{\theta}$ denote the so–called axial vectors. Pull–back of the covariant basis vectors with the rotation tensors $\mathbf{R}_0 = \mathbf{A}_i \otimes \mathbf{e}_i$ and $\mathbf{R} = \mathbf{a}_i \otimes \mathbf{e}_i$ yields

$$\begin{aligned} \mathbf{F}_1 &:= \mathbf{R}_0^T \mathbf{G}_1 = \boldsymbol{\varepsilon}_0 + \boldsymbol{\kappa}_0 \times \mathbf{d} & \mathbf{f}_1 &:= \mathbf{R}^T \mathbf{g}_1 = \boldsymbol{\varepsilon} + \boldsymbol{\kappa} \times \mathbf{d} + \alpha' \bar{w} \mathbf{e}_1 \\ \mathbf{F}_2 &:= \mathbf{R}_0^T \mathbf{G}_2 = \mathbf{e}_2 & \mathbf{f}_2 &:= \mathbf{R}^T \mathbf{g}_2 = \mathbf{e}_2 + \alpha \bar{w}_{,2}\, \mathbf{e}_1 \\ \mathbf{F}_3 &:= \mathbf{R}_0^T \mathbf{G}_3 = \mathbf{e}_3 & \mathbf{f}_3 &:= \mathbf{R}^T \mathbf{g}_3 = \mathbf{e}_3 + \alpha \bar{w}_{,3}\, \mathbf{e}_1 \end{aligned} \tag{7}$$

with $\mathbf{d} = \xi_2\mathbf{e}_2 + \xi_3\mathbf{e}_3$. The strain vectors of the current configuration are defined with

$$\boldsymbol{\varepsilon} := \mathbf{R}^T\mathbf{x}_0' = \begin{bmatrix} \mathbf{x}_0' \cdot \mathbf{a}_1 \\ \mathbf{x}_0' \cdot \mathbf{a}_2 \\ \mathbf{x}_0' \cdot \mathbf{a}_3 \end{bmatrix} \qquad \boldsymbol{\kappa} := \mathbf{R}^T\boldsymbol{\theta} = \begin{bmatrix} \mathbf{a}_2' \cdot \mathbf{a}_3 \\ \mathbf{a}_3' \cdot \mathbf{a}_1 \\ \mathbf{a}_1' \cdot \mathbf{a}_2 \end{bmatrix} . \tag{8}$$

The corresponding quantities of the reference configuration read $\boldsymbol{\varepsilon}_0 = \mathbf{R}_0^T\mathbf{X}_0'$ and $\boldsymbol{\kappa}_0 = \mathbf{R}_0^T\boldsymbol{\theta}_0$.
Eqs. (6) are inserted into the Green–Lagrangian strain tensor $\mathbf{E} = E_{ij}\mathbf{G}^i \otimes \mathbf{G}^j$, where the dual basis vectors $\mathbf{G}^i$ are defined in a standard way $\mathbf{G}_i \cdot \mathbf{G}^j = \delta_i^j$. The components which contribute to the virtual work read

$$\mathbf{E} = \begin{bmatrix} E_{11} \\ 2E_{12} \\ 2E_{13} \end{bmatrix} = \begin{bmatrix} \frac{1}{2}(g_{11} - G_{11}) \\ g_{12} - G_{12} \\ g_{13} - G_{13} \end{bmatrix} \tag{9}$$

with the metric coefficients

$$\begin{aligned} G_{ij} &= \mathbf{G}_i \cdot \mathbf{G}_j = \mathbf{G}_i \cdot \mathbf{R}_0\mathbf{R}_0^T\mathbf{G}_j = \mathbf{F}_i \cdot \mathbf{F}_j \\ g_{ij} &= \mathbf{g}_i \cdot \mathbf{g}_j = \mathbf{g}_i \cdot \mathbf{R}\mathbf{R}^T\mathbf{g}_j = \mathbf{f}_i \cdot \mathbf{f}_j \end{aligned} \tag{10}$$

of the reference configuration and current configuration, respectively.

3 VARIATIONAL FORMULATION OF THE BOUNDARY VALUE PROBLEM

In this section the virtual work of the stresses and the external forces are derived considering the beam kinematic. For this purpose stress resultants are defined. The associated Euler–Lagrange equations and the linearization of the virtual work expressions are given.

3.1 Internal Virtual Work and Definition of Stress Resultants

Volume forces $\rho_0\bar{\mathbf{b}}$ and applied surface loads $\bar{\mathbf{t}}$ are acting on the considered body. Hence the equilibrium is given here in weak form

$$g(\mathbf{v}, \delta\mathbf{v}) = \int_{\mathcal{B}_0} \mathbf{S} \cdot \delta\mathbf{E}\, \mathrm{d}V - \int_{\mathcal{B}_0} \rho_0\bar{\mathbf{b}} \cdot \delta\mathbf{u}\, \mathrm{d}V - \int_{\partial\mathcal{B}_0} \bar{\mathbf{t}} \cdot \delta\mathbf{u}\, \mathrm{d}\Omega = 0\,. \tag{11}$$

The independent kinematic quantities of the beam are $\mathbf{v} = [\mathbf{u}, \mathbf{R}, \alpha]^T$, where $\mathbf{u} = \mathbf{x}_0 - \mathbf{X}_0$ and $\mathbf{R} = \mathbf{a}_i \otimes \mathbf{e}_i$ denote the displacement vector and the rotation tensor of the reference curve according to (2), respectively. The space of kinematically admissible variations is introduced by

$$\mathcal{V} := \{\delta\mathbf{v} = [\delta\mathbf{u}, \delta\mathbf{w}, \delta\alpha]^T : [0, L] \longrightarrow R^3 | \quad \delta\mathbf{v} = \mathbf{0} \quad \text{on} \quad \mathcal{S}_u\} \tag{12}$$

where $\mathcal{S}_u$ describes the boundaries with prescribed displacements and rotations. Here, the axial vector $\delta\mathbf{w}$ is defined by $\delta\mathbf{a}_i = \delta\mathbf{R}\mathbf{R}^T\,\mathbf{a}_i = \delta\mathbf{w} \times \mathbf{a}_i$.
The Green–Lagrangian strain tensor is work conjugate to the Second Piola–Kirchhoff stress tensor $\mathbf{S} = S^{ij}\,\mathbf{G}_i \otimes \mathbf{G}_j$. Within the present beam theory the components S^{22}, S^{33}, S^{23}

are neglected. Using matrix notation the vector of non–vanishing stress components is defined

$$\mathbf{S} = \left[S^{11}, S^{12}, S^{13}\right]^T . \tag{13}$$

The variation of the work conjugate Green–Lagrangian strains (9) yields with (7) – (10)

$$\delta\mathbf{E} = \begin{bmatrix} \delta E_{11} \\ 2\delta E_{12} \\ 2\delta E_{13} \end{bmatrix} = \begin{bmatrix} \mathbf{f}_1 \cdot \delta\mathbf{f}_1 \\ \mathbf{f}_2 \cdot \delta\mathbf{f}_1 + \mathbf{f}_1 \cdot \delta\mathbf{f}_2 \\ \mathbf{f}_3 \cdot \delta\mathbf{f}_1 + \mathbf{f}_1 \cdot \delta\mathbf{f}_3 \end{bmatrix} \tag{14}$$

where

$$\begin{aligned} \delta\mathbf{f}_1 &= \delta\boldsymbol{\varepsilon} + \delta\boldsymbol{\kappa} \times \mathbf{d} + \delta\alpha'\, \bar{w}\mathbf{e}_1 \\ \delta\mathbf{f}_2 &= \delta\alpha\, \bar{w}_{,2}\, \mathbf{e}_1 \\ \delta\mathbf{f}_3 &= \delta\alpha\, \bar{w}_{,3}\, \mathbf{e}_1 . \end{aligned} \tag{15}$$

Introducing

$$\begin{aligned} \hat{\mathbf{F}} &= [\mathbf{f}_1,\, \mathbf{f}_2,\, \mathbf{f}_3] \\ \mathbf{W}_d &= \operatorname{skew}\mathbf{d} = \begin{bmatrix} 0 & -\xi_3 & \xi_2 \\ \xi_3 & 0 & 0 \\ -\xi_2 & 0 & 0 \end{bmatrix} \\ \mathbf{a} &= (\mathbf{f}_1 \cdot \mathbf{e}_1)\,(\bar{w}_{,2}\, \mathbf{e}_2 + \bar{w}_{,3}\, \mathbf{e}_3) \end{aligned} \tag{16}$$

one obtains

$$\begin{aligned} \delta\mathbf{E} &= \mathbf{A}\, \delta\hat{\mathbf{E}} \\ \mathbf{A} &= [\hat{\mathbf{F}}^T,\, \hat{\mathbf{F}}^T\mathbf{W}_d^T,\, \mathbf{a},\, \bar{w}\, \hat{\mathbf{F}}^T\mathbf{e}_1] \qquad\qquad \delta\hat{\mathbf{E}} = \begin{bmatrix} \delta\boldsymbol{\varepsilon} \\ \delta\boldsymbol{\kappa} \\ \delta\alpha \\ \delta\alpha' \end{bmatrix} . \end{aligned} \tag{17}$$

The variation of the beam strains (8) yields

$$\begin{aligned} \delta\boldsymbol{\varepsilon} &= \mathbf{R}^T\delta\mathbf{x}_0' + \delta\mathbf{R}^T\mathbf{x}_0' = \mathbf{R}^T(\delta\mathbf{x}_0' - \delta\mathbf{w} \times \mathbf{x}_0') \\ \delta\boldsymbol{\kappa} &= \mathbf{R}^T\delta\boldsymbol{\theta} + \delta\mathbf{R}^T\boldsymbol{\theta} = \mathbf{R}^T\delta\mathbf{w}' . \end{aligned} \tag{18}$$

Eq. $(18)_1$ is evident, whereas a proof of $(18)_2$ is given e.g. in [17]. Furthermore a representation of the components yields

$$\delta\boldsymbol{\varepsilon} = \begin{bmatrix} \mathbf{a}_1 \cdot \delta\mathbf{u}' + \mathbf{x}_0' \cdot \delta\mathbf{a}_1 \\ \mathbf{a}_2 \cdot \delta\mathbf{u}' + \mathbf{x}_0' \cdot \delta\mathbf{a}_2 \\ \mathbf{a}_3 \cdot \delta\mathbf{u}' + \mathbf{x}_0' \cdot \delta\mathbf{a}_3 \end{bmatrix} \qquad \delta\boldsymbol{\kappa} = \begin{bmatrix} \mathbf{a}_3 \cdot \delta\mathbf{a}_2' + \mathbf{a}_2' \cdot \delta\mathbf{a}_3 \\ \mathbf{a}_1 \cdot \delta\mathbf{a}_3' + \mathbf{a}_3' \cdot \delta\mathbf{a}_1 \\ \mathbf{a}_2 \cdot \delta\mathbf{a}_1' + \mathbf{a}_1' \cdot \delta\mathbf{a}_2 \end{bmatrix} . \tag{19}$$

Using (17) the internal virtual work in (11) can be rewritten with $\mathrm{d}V = \mathrm{d}A\,\mathrm{d}S$ as

$$\begin{aligned} g_{int}(\mathbf{v}, \delta\mathbf{v}) &= \int_{\mathcal{B}_0} \delta\mathbf{E}^T\, \mathbf{S}\, \mathrm{d}V = \int_S \delta\hat{\mathbf{E}}^T\hat{\mathbf{S}}\, \mathrm{d}S \\ &= \int_S (\mathbf{F} \cdot \delta\boldsymbol{\varepsilon} + \mathbf{M} \cdot \delta\boldsymbol{\kappa} + F^w\delta\alpha + M^w\delta\alpha')\, \mathrm{d}S \end{aligned} \tag{20}$$

with the vector of stress resultants

$$\hat{\mathbf{S}} = \int_A \mathbf{A}^T\,\mathbf{S}\,\mathrm{d}A = \begin{bmatrix} \mathbf{F} \\ \mathbf{M} \\ F^w \\ M^w \end{bmatrix} = \int_A \begin{bmatrix} \mathbf{T} \\ \mathbf{L} \\ T^w \\ L^w \end{bmatrix} \mathrm{d}A \tag{21}$$

where $\mathbf{T} = [T^{11},\, T^{12},\, T^{13}]^T = \hat{\mathbf{F}}\mathbf{S}$ and $\mathbf{L} = \mathbf{W}_d\,\mathbf{T}$. Finally a component representation of the vector of stress resultants yields

$$\hat{\mathbf{S}} = \begin{bmatrix} F^1 \\ F^2 \\ F^3 \\ M^1 \\ M^2 \\ M^3 \\ F^w \\ M^w \end{bmatrix} = \int_A \begin{bmatrix} T^{11} \\ T^{12} \\ T^{13} \\ T^{13}\xi_2 - T^{12}\xi_3 \\ T^{11}\xi_3 \\ -T^{11}\xi_2 \\ \tilde{T}^{12}\bar{w}_{,2} + \tilde{T}^{13}\bar{w}_{,3} \\ T^{11}\bar{w} \end{bmatrix} \mathrm{d}A \tag{22}$$

with $\tilde{T}^{1\alpha} = (\mathbf{f}_1 \cdot \mathbf{e}_1) S^{1\alpha}$ and $\alpha = 2, 3$. Herein, F^1 is the normal force, F^2 and F^3 the shear forces, M^1 the torsion moment, M^2 and M^3 the bending moments, F^w the bi–shear and M^w the bi–moment, respectively.

3.2 External Virtual Work and Euler–Lagrange Equations

In this paper the volume forces $\rho_0\bar{\mathbf{b}}$ and the surface loads $\bar{\mathbf{t}}$ according to (11) are considered with the load $\bar{\mathbf{p}} = \bar{\mathbf{p}}(S)$ acting at the coordinates $\{p_2,\, p_3\}$, see Fig.1. The vector of the loading point in the current configuration reads $\mathbf{x}_p = \mathbf{x}_0 + \mathbf{r}_p$ with $\mathbf{r}_p = p_2\mathbf{a}_2 + p_3\mathbf{a}_3 + \alpha\,\bar{w}_p\,\mathbf{a}_1$ and $\bar{w}_p = \bar{w}(p_2, p_3)$.
Hence the external virtual work reads

$$\begin{aligned} g_{ext}(\mathbf{v}, \delta\mathbf{v}) &= -\int_S \bar{\mathbf{p}} \cdot \delta\mathbf{x}_p\,\mathrm{d}S \\ &= -\int_S \bar{\mathbf{p}} \cdot (\delta\mathbf{x}_0 + p_2\delta\mathbf{a}_2 + p_3\delta\mathbf{a}_3 + \alpha\bar{w}_p\delta\mathbf{a}_1 + \delta\alpha\bar{w}_p\mathbf{a}_1)\,\mathrm{d}S \\ &= -\int_S (\bar{\mathbf{p}} \cdot \delta\mathbf{x}_0 + \bar{\mathbf{m}} \cdot \delta\mathbf{w} + \bar{p}_1\delta\alpha)\,\mathrm{d}S \end{aligned} \tag{23}$$

with $\bar{\mathbf{m}} = \mathbf{r}_p \times \bar{\mathbf{p}}$ and $\bar{p}_1 = \bar{w}_p\,(\bar{\mathbf{p}} \cdot \mathbf{a}_1)$.

The weak form of equilibrium (11) is now reformulated using the expressions (20), (18) and (23). This yields

$$g(\mathbf{v}, \delta\mathbf{v}) = \int_S [\mathbf{f} \cdot (\delta\mathbf{x}_0' - \delta\mathbf{w} \times \mathbf{x}_0') + \mathbf{m} \cdot \delta\mathbf{w}' + F^w\delta\alpha + M^w\delta\alpha' - (\bar{\mathbf{p}} \cdot \delta\mathbf{x}_0 + \bar{\mathbf{m}} \cdot \delta\mathbf{w} + \bar{p}_1\delta\alpha)]\,\mathrm{d}S = 0 \tag{24}$$

with $\mathbf{f} := \mathbf{RF}$ and $\mathbf{m} := \mathbf{RM}$. Next, integration by parts yields with homogeneous stress boundary conditions

$$g(\mathbf{v}, \delta\mathbf{v}) = -\int_S [(\mathbf{f}' + \bar{\mathbf{p}}) \cdot \delta\mathbf{x}_0 + (\mathbf{m}' + \mathbf{x}_0' \times \mathbf{f} + \bar{\mathbf{m}}) \cdot \delta\mathbf{w} + (M^{w\prime} - F^w + \bar{p}_1)\, \delta\alpha]\, \mathrm{d}S = 0\,. \tag{25}$$

Applying standard arguments from variational calculus we obtain

$$\begin{aligned} \mathbf{f}' + \bar{\mathbf{p}} &= \mathbf{0} \\ \mathbf{m}' + \mathbf{x}_0' \times \mathbf{f} + \bar{\mathbf{m}} &= \mathbf{0} \\ M^{w\prime} - F^w + \bar{p}_1 &= 0\,. \end{aligned} \tag{26}$$

These are the Euler–Lagrange equations of the variational formulation. The first two equations in (26) are well–known equilibrium equations of a three–dimensional beam using a vector notation. The third equation is identical to that of the linear theory. Reissner [12] derived $(26)_3$ in the context of a second–order geometrical nonlinear theory.

3.3 Linearization of the Virtual Work Expressions

For the subsequent finite element formulation we need to derive the linearization of the weak form of equilibrium (11). This is formally achieved using the directional derivative

$$L\,[g(\mathbf{v}, \delta\mathbf{v})] = g + \mathrm{D}g \cdot \Delta\mathbf{v}\,, \qquad \mathrm{D}g \cdot \Delta\mathbf{v} = \frac{\mathrm{d}}{\mathrm{d}\varepsilon}\,[G(\mathbf{v} + \varepsilon\Delta\mathbf{v})]_{\varepsilon=0} \tag{27}$$

where $\Delta\mathbf{v} = [\Delta\mathbf{u}, \Delta\mathbf{w}, \Delta\alpha]^T$. The linearization of the internal virtual work yields a material part and a geometrical part

$$\mathrm{D}g_{int}(\mathbf{v}, \delta\mathbf{v}) \cdot \Delta\mathbf{v} = \int_S (\delta\hat{\mathbf{E}}^T \hat{\mathbf{D}} \Delta\hat{\mathbf{E}} + \Delta\delta\hat{\mathbf{E}}^T\, \hat{\mathbf{S}})\, \mathrm{d}S\,. \tag{28}$$

Here the linearized beam strains $\Delta\hat{\mathbf{E}} = [\Delta\boldsymbol{\varepsilon}, \Delta\boldsymbol{\kappa}, \Delta\alpha, \Delta\alpha']^T$ are obtained from (19) replacing the operator δ by Δ. Furthermore the linearized virtual strains are expressed by $\Delta\delta\hat{\mathbf{E}} = [\Delta\delta\boldsymbol{\varepsilon}, \Delta\delta\boldsymbol{\kappa}, 0, 0]^T$ with

$$\begin{aligned} \Delta\delta\boldsymbol{\varepsilon} &= \begin{bmatrix} \delta\mathbf{u}' \cdot \Delta\mathbf{a}_1 + \delta\mathbf{a}_1 \cdot \Delta\mathbf{u}' + \mathbf{x}_0' \cdot \Delta\delta\mathbf{a}_1 \\ \delta\mathbf{u}' \cdot \Delta\mathbf{a}_2 + \delta\mathbf{a}_2 \cdot \Delta\mathbf{u}' + \mathbf{x}_0' \cdot \Delta\delta\mathbf{a}_2 \\ \delta\mathbf{u}' \cdot \Delta\mathbf{a}_3 + \delta\mathbf{a}_1 \cdot \Delta\mathbf{u}' + \mathbf{x}_0' \cdot \Delta\delta\mathbf{a}_3 \end{bmatrix} \\ \Delta\delta\boldsymbol{\kappa} &= \begin{bmatrix} \delta\mathbf{a}_2' \cdot \Delta\mathbf{a}_3 + \delta\mathbf{a}_3 \cdot \Delta\mathbf{a}_2' + \mathbf{a}_3 \cdot \Delta\delta\mathbf{a}_2' + \mathbf{a}_2' \cdot \Delta\delta\mathbf{a}_3 \\ \delta\mathbf{a}_3' \cdot \Delta\mathbf{a}_1 + \delta\mathbf{a}_1 \cdot \Delta\mathbf{a}_3' + \mathbf{a}_1 \cdot \Delta\delta\mathbf{a}_3' + \mathbf{a}_3' \cdot \Delta\delta\mathbf{a}_1 \\ \delta\mathbf{a}_1' \cdot \Delta\mathbf{a}_2 + \delta\mathbf{a}_2 \cdot \Delta\mathbf{a}_1' + \mathbf{a}_2 \cdot \Delta\delta\mathbf{a}_1' + \mathbf{a}_1' \cdot \Delta\delta\mathbf{a}_2 \end{bmatrix}. \end{aligned} \tag{29}$$

Next the linearization of the stress resultants (21) applying the product rule leads to

$$\hat{\mathbf{D}} = \frac{\mathrm{d}\,\hat{\mathbf{S}}}{\mathrm{d}\,\hat{\mathbf{E}}} = \frac{\mathrm{d}}{\mathrm{d}\,\hat{\mathbf{E}}}[\int_A \mathbf{A}^T\, \mathbf{S}\, \mathrm{d}A] = \int_A (\mathbf{A}^T \mathbf{C}_T \mathbf{A} + \hat{\mathbf{G}})\, \mathrm{d}A\,. \tag{30}$$

The first part follows from differentiation of the stress vector $\mathbf{S}$ and the incremental Green–Lagrangian strains $\mathrm{d}\mathbf{E} = \mathbf{A}\, \mathrm{d}\hat{\mathbf{E}}$. The tangential matrix $\mathbf{C}_T := \mathrm{d}\mathbf{S}/\mathrm{d}\mathbf{E}$ is specified

for elastic–plastic material behaviour in the next section. The second part follows from differentiation of the matrix product $\mathbf{A}^T\mathbf{S}$ where the stress vector $\mathbf{S}$ is held fixed. With

$$\begin{bmatrix} \mathbf{T} \\ \mathbf{L} \\ T^w \\ L^w \end{bmatrix} = \begin{bmatrix} S^{11}\mathbf{f}_1 + S^{12}\mathbf{f}_2 + S^{13}\mathbf{f}_3 \\ \mathbf{W}_d(S^{11}\mathbf{f}_1 + S^{12}\mathbf{f}_2 + S^{13}\mathbf{f}_3) \\ \tilde{S}(\mathbf{f}_1 \cdot \mathbf{e}_1) \\ S^{11}\bar{w}(\mathbf{f}_1 \cdot \mathbf{e}_1) + \tilde{S}\alpha\bar{w} \end{bmatrix} \tag{31}$$

where $\tilde{S} = S^{12}\bar{w}_{,2} + S^{13}\bar{w}_{,3}$ and $\mathbf{f}_i$ according to (7) one obtains

$$\hat{\mathbf{G}} = \begin{bmatrix} \frac{\partial \mathbf{T}}{\partial \boldsymbol{\varepsilon}} & \frac{\partial \mathbf{T}}{\partial \boldsymbol{\kappa}} & \frac{\partial \mathbf{T}}{\partial \alpha} & \frac{\partial \mathbf{T}}{\partial \alpha'} \\ \frac{\partial \mathbf{L}}{\partial \boldsymbol{\varepsilon}} & \frac{\partial \mathbf{L}}{\partial \boldsymbol{\kappa}} & \frac{\partial \mathbf{L}}{\partial \alpha} & \frac{\partial \mathbf{L}}{\partial \alpha'} \\ (\frac{\partial T^w}{\partial \boldsymbol{\varepsilon}})^T & (\frac{\partial T^w}{\partial \boldsymbol{\kappa}})^T & \frac{\partial T^w}{\partial \alpha} & \frac{\partial T^w}{\partial \alpha'} \\ (\frac{\partial L^w}{\partial \boldsymbol{\varepsilon}})^T & (\frac{\partial L^w}{\partial \boldsymbol{\kappa}})^T & \frac{\partial L^w}{\partial \alpha} & \frac{\partial L^w}{\partial \alpha'} \end{bmatrix} = \begin{bmatrix} S^{11}\mathbf{1} & S^{11}\mathbf{W}_d^T & \tilde{S}\mathbf{e}_1 & S^{11}\bar{w}\mathbf{e}_1 \\ S^{11}\mathbf{W}_d & -S^{11}\mathbf{W}_d^2 & \tilde{S}\tilde{\mathbf{d}} & S^{11}\bar{w}\tilde{\mathbf{d}} \\ \tilde{S}\mathbf{e}_1^T & \tilde{S}\tilde{\mathbf{d}}^T & 0 & \tilde{S}\bar{w} \\ S^{11}\bar{w}\mathbf{e}_1^T & S^{11}\bar{w}\tilde{\mathbf{d}}^T & \tilde{S}\bar{w} & S^{11}\bar{w}^2 \end{bmatrix} \tag{32}$$

where $\tilde{\mathbf{d}} = \mathbf{W}_d\mathbf{e}_1 = \xi_3\mathbf{e}_2 - \xi_2\mathbf{e}_3$. The integration over the cross–section in (21) and (30) is performed numerically. The warping function $\bar{w}$ is determined for arbitrary cross–sections in a separate computing process using the finite element method as is discussed in [16]. The finite element mesh for the computation of $\bar{w}$ is used here to perform the numerical Gauss integration. In case of small strains $\hat{\mathbf{F}} \approx \mathbf{1}$ holds, $\mathbf{A}$ becomes independent of the displacement field and $\hat{\mathbf{G}}$ vanishes.
Finally we derive the linearization of the external virtual work as

$$\mathrm{D}g_{ext}(\mathbf{v}, \delta\mathbf{v}) \cdot \Delta\mathbf{v} \;=\; -\int_S \bar{\mathbf{p}} \cdot \Delta\delta\mathbf{x}_p \, \mathrm{d}S \tag{33}$$

with $\Delta\delta\mathbf{x}_p = p_2\Delta\delta\mathbf{a}_2 + p_3\Delta\delta\mathbf{a}_3 + \alpha\bar{w}_p\Delta\delta\mathbf{a}_1 + \delta\alpha\bar{w}_p\Delta\mathbf{a}_1 + \Delta\alpha\bar{w}_p\delta\mathbf{a}_1$.

4 MATERIAL LAW AND STRESS RESULTANTS

In this section we present the constitutive equations for elastoplastic material behaviour. We consider metallic materials which can be described by the von Mises yield criterion with isotropic hardening and associated flow rule. For elasticity the section integrals are reformulated using the equations of Saint–Venant's torsion theory and Green's theorem. This yields an elasticity matrix where for the general case torsion bending coupling occurs.

4.1 Elastic–Plastic Stress Analysis

The Green–Lagrangian strains (9) are decomposed in an elastic and plastic part

$$\mathbf{E} = \mathbf{E}^{el} + \mathbf{E}^{pl} \tag{34}$$

which holds for small elastic and plastic strains. The elastic part is described by the so–called St.Venant–Kirchhoff material law. Thus, a quadratic strain energy function is postulated where the stresses are obtained by partial derivatives

$$W_s(\mathbf{E}^{el}) = \frac{1}{2}\mathbf{E}^{elT}\mathbf{C}\mathbf{E}^{el}\,, \qquad\qquad \mathbf{S} = \frac{\partial W_s}{\partial \mathbf{E}^{el}} = \mathbf{C}\,\mathbf{E}^{el}. \tag{35}$$

Since the stresses S^{22}, S^{33} and S^{23} are neglected the constitutive matrix reads

$$\mathbf{C} = \begin{bmatrix} E & 0 & 0 \\ 0 & G & 0 \\ 0 & 0 & G \end{bmatrix}. \tag{36}$$

Here, E and G denote Young's modulus and shear modulus, respectively.
The plastic flow of metals can be described using the von Mises yield condition with isotropic hardening

$$F(\mathbf{S}, e^{pl}) = h(\mathbf{S}) - y_0 + r(e^{pl}) \tag{37}$$

where

$$h(\mathbf{S}) = \sqrt{\mathbf{S}^T \mathbf{P} \mathbf{S}}\,, \qquad \mathbf{P} = \begin{bmatrix} 1 & 0 & 0 \\ 0 & 3 & 0 \\ 0 & 0 & 3 \end{bmatrix}. \tag{38}$$

Assuming strain hardening the yield stress y is given here with the equivalent plastic strain e^{pl} using a linear hardening function $r(e^{pl}) = -K\, e^{pl}$, thus

$$y = y_0 + K\, e^{pl}\,. \tag{39}$$

The initial yield stress y_0 and the hardening parameter K are material constants.
The rates of the plastic strains and of the equivalent plastic strain are described using an associated flow rule

$$\dot{\mathbf{E}}^{pl} = \dot{\lambda} \frac{\partial F}{\partial \mathbf{S}} \qquad \dot{e}^{pl} = \dot{\lambda} \frac{\partial F}{\partial r}\,, \tag{40}$$

where the gradient of the yield condition can be expressed as

$$\frac{\partial F}{\partial \mathbf{S}} = \frac{1}{h} \mathbf{P}\mathbf{S} := \mathbf{N} \qquad \frac{\partial F}{\partial r} = 1\,. \tag{41}$$

In (40) the loading–unloading conditions

$$\dot{\lambda} \geq 0\,, \qquad F \leq 0\,, \qquad \dot{\lambda}\, F = 0 \tag{42}$$

must hold.
Hence, a backward Euler integration algorithm within a time step $t_{n+1} = t_n + \Delta t$ leads to

$$\begin{aligned} \mathbf{E}^{pl}_{n+1} &= \mathbf{E}^{pl}_n + \gamma \mathbf{N}_{n+1} \\ e^{pl}_{n+1} &= e^{pl}_n + \gamma \end{aligned} \tag{43}$$

where $\gamma = \int_{t_n}^{t_{n+1}} \dot{\lambda}\, \mathrm{d}t$. Inserting $(35)_2$ and $(43)_1$ into (34) at time t_{n+1} yields

$$\mathbf{S}_{n+1}(\gamma) = \bar{\mathbf{C}}(\gamma)\, \mathbf{E}^{tr} \qquad \mathbf{E}^{tr} := \mathbf{E}_{n+1} - \mathbf{E}^{pl}_n \tag{44}$$

with

$$\bar{\mathbf{C}}(\gamma) = (\mathbf{C}^{-1} + \frac{\gamma}{y}\mathbf{P})^{-1} = \begin{bmatrix} \frac{E}{1+E\gamma/y} & 0 & 0 \\ 0 & \frac{G}{1+3G\gamma/y} & 0 \\ 0 & 0 & \frac{G}{1+3G\gamma/y} \end{bmatrix}. \tag{45}$$

To express $\mathbf{S}_{n+1}$ as an explicit function of γ we replaced $h(\mathbf{S})$ by $y(\gamma)$ in (45) using $F(\mathbf{S}, e^{pl}) = 0$. The consistency parameter γ is obtained with the solution of the yield

condition $F(\mathbf{S}_{n+1}, e^{pl}_{n+1}) = 0$. This is achieved iteratively within a Newton iteration procedure

$$\begin{aligned} \gamma^{(l+1)} &= \gamma^{(l)} - \frac{F^{(l)}}{\frac{\mathrm{d}F^{(l)}}{\mathrm{d}\gamma}} \\ F^{(l)} &= h\left[\mathbf{S}_{n+1}(\gamma^{(l)})\right] - y\left[e^{pl}_{n+1}(\gamma^{(l)})\right] \\ \frac{\mathrm{d}F^{(l)}}{\mathrm{d}\gamma} &= -\left[\frac{h}{y}(1 - \frac{\gamma}{y}\frac{\mathrm{d}y}{\mathrm{d}e^{pl}})\,\mathbf{N}^T\bar{\mathbf{C}}\mathbf{N} + \frac{\mathrm{d}y}{\mathrm{d}e^{pl}}\right] \end{aligned} \tag{46}$$

where l denotes the iteration number and $\mathrm{d}y/\mathrm{d}e^{pl} = K$. As starting value we take $\gamma^{(0)} = 0$. The equivalent plastic strain follows from $(43)_2$. Note, that during the iteration $y \neq h$ holds. The elastoplastic stresses at each integration point are evaluated using a well–known operator split method. The predictor step yields the so–called trial stresses $\mathbf{S}^{tr} = \mathbf{C}\,\mathbf{E}^{tr}$. If above yield condition is not fulfilled the stresses are given with the corrector step according to (44), thus

$$\mathbf{S}_{n+1} = \begin{cases} \mathbf{C}\,\mathbf{E}^{tr} & \text{if} \quad F(\mathbf{S}^{tr}, e^{pl}_n) \leq 0 \\ \bar{\mathbf{C}}\,\mathbf{E}^{tr} & \text{if} \quad F(\mathbf{S}^{tr}, e^{pl}_n) > 0\,. \end{cases} \tag{47}$$

The consistency parameter γ depends on the strains $\mathbf{E}$ via eq. $(46)_2$. This has to be considered when linearizing the stress vector (47). One obtains

$$\left.\frac{\mathrm{d}\mathbf{S}}{\mathrm{d}\mathbf{E}}\right|_{n+1} = \begin{cases} \mathbf{C} & \text{if} \quad F(\mathbf{S}^{tr}, e^{pl}_n) \leq 0 \\ \bar{\mathbf{C}} - \dfrac{\bar{\mathbf{C}}\mathbf{N}\mathbf{N}^T\bar{\mathbf{C}}}{\mathbf{N}^T\bar{\mathbf{C}}\mathbf{N} + \beta} & \text{if} \quad F(\mathbf{S}^{tr}, e^{pl}_n) > 0 \end{cases} \tag{48}$$

with $\beta = K/(1 - \gamma K/y)$.

4.2 Elastic Stress Analysis

In case of small strains the transformation matrix $\hat{\mathbf{F}}$ according to (16) is approximately the identity matrix, thus $\hat{\mathbf{F}} \approx \mathbf{1}$. In this case $\mathbf{A}$ is given with (17)

$$\mathbf{A} = \begin{bmatrix} 1 & 0 & 0 & 0 & \xi_3 & -\xi_2 & 0 & \bar{w} \\ 0 & 1 & 0 & -\xi_3 & 0 & 0 & \bar{w}_{,2} & 0 \\ 0 & 0 & 1 & \xi_2 & 0 & 0 & \bar{w}_{,3} & 0 \end{bmatrix}. \tag{49}$$

One can see that $\mathbf{A}$ does not depend on the deformation and $\mathbf{E} = \mathbf{A}\hat{\mathbf{E}}$ holds. For elasticity the stress vector is obtained from $\mathbf{S} = \mathbf{C}\mathbf{A}\hat{\mathbf{E}}$. Now the matrix of the linearized stress resultants (30) can be reformulated using (48), (36), (49) and $\hat{\mathbf{G}} = \mathbf{0}$

$$\hat{\mathbf{D}} = \int_A \begin{bmatrix} E & 0 & 0 & 0 & E\xi_3 & -E\xi_2 & 0 & E\bar{w} \\ & G & 0 & -G\xi_3 & 0 & 0 & G\bar{w}_{,2} & 0 \\ & & G & G\xi_2 & 0 & 0 & G\bar{w}_{,3} & 0 \\ & & & G(\xi_2^2 + \xi_3^2) & 0 & 0 & G(\xi_2\bar{w}_{,3} - \xi_3\bar{w}_{,2}) & 0 \\ & & & & E\xi_3^2 & -E\xi_2\xi_3 & 0 & E\bar{w}\xi_3 \\ & & & & & E\xi_2^2 & 0 & -E\bar{w}\xi_2 \\ & & & \text{sym} & & & G(\bar{w}_{,2}^2 + \bar{w}_{,3}^2) & 0 \\ & & & & & & & E\bar{w}^2 \end{bmatrix} \mathrm{d}A\,. \tag{50}$$

The centroid of the cross–section with coordinates $\{s_2, s_3\}$ is denoted by S, see Fig. 1. Furthermore we denote the area of the cross–section by A, the moments of inertia relative to the centroid by $\bar{I}_{22}, \bar{I}_{33}, \bar{I}_{23}$, the Saint–Venant torsion modulus by I_T and the warping constant by $I_{\tilde{w}}$. The following definitions are given with $\alpha, \beta = 2, 3$

$$\begin{aligned}
S_\alpha &:= \int_A \xi_\alpha \mathrm{d}A = A s_\alpha \\
\bar{I}_{\alpha\beta} &:= \int_A \bar{\xi}_\alpha \bar{\xi}_\beta \,\mathrm{d}A \qquad\qquad I_{\alpha\beta} := \int_A \xi_\alpha \xi_\beta \,\mathrm{d}A = \bar{I}_{\alpha\beta} + A s_\alpha s_\beta \\
I_0 &:= I_{22} + I_{33} \\
I_T &:= \int_A [\xi_2(\bar{w}_{,3} + \xi_2) - \xi_3(\bar{w}_{,2} - \xi_3)] \,\mathrm{d}A = I_0 + \int_A (\xi_2 \bar{w}_{,3} - \xi_3 \bar{w}_{,2}) \,\mathrm{d}A \\
I_{\tilde{w}} &:= \int_A \tilde{w}^2 \,\mathrm{d}A \,.
\end{aligned} \tag{51}$$

Using the equations of Saint–Venants torsion theory (3) and application of Green's theorem yields after some algebra the missing quantities, see appendix A.1

$$\begin{aligned}
\int_A \bar{w}_{,2} \,\mathrm{d}A &= A s_3 \qquad \int_A \bar{w}_{,3} \,\mathrm{d}A = -A s_2 \\
\int_A (\bar{w}_{,2}^2 + \bar{w}_{,3}^2) \,\mathrm{d}A &= I_0 - I_T \\
\int_A \bar{w} \xi_2 \,\mathrm{d}A &= \bar{I}_{22} m_3 - \bar{I}_{23} m_2 := I_{\bar{w}2} \qquad \int_A \bar{w} \xi_3 \,\mathrm{d}A = -\bar{I}_{33} m_2 + \bar{I}_{23} m_3 := I_{\bar{w}3} \\
\int_A \bar{w}^2 \,\mathrm{d}A &= I_{\tilde{w}} + \bar{I}_{33} m_2^2 + \bar{I}_{22} m_3^2 - 2 \bar{I}_{23} m_2 m_3 := I_{\bar{w}} \,.
\end{aligned} \tag{52}$$

A numerical computation of $\bar{w}(\xi_2, \xi_3)$ which fulfills $\int_A \bar{w} \,\mathrm{d}A = 0$ and above section quantities for arbitrary cross–sections using the finite element method is discussed in e.g. [16]. In fact $(52)_4$ and $(52)_5$ are two equations which can be solved for the coordinates m_2 and m_3 if $I_{\bar{w}2}$ and $I_{\bar{w}3}$ are known, see Ref. [16].
Now, (50) can be expressed inserting the section quantities (51) and (52) as follows

$$\hat{\mathbf{D}} = \begin{bmatrix}
EA & 0 & 0 & 0 & EAs_3 & -EAs_2 & 0 & 0 \\
 & GA & 0 & -GAs_3 & 0 & 0 & GAs_3 & 0 \\
 & & GA & GAs_2 & 0 & 0 & -GAs_2 & 0 \\
 & & & GI_0 & 0 & 0 & -G(I_0 - I_T) & 0 \\
 & & & & EI_{33} & -EI_{23} & 0 & EI_{\bar{w}3} \\
 & & & & & EI_{22} & 0 & -EI_{\bar{w}2} \\
 & & & \text{sym} & & & G(I_0 - I_T) & 0 \\
 & & & & & & & EI_{\bar{w}}
\end{bmatrix}. \tag{53}$$

The elasticity matrix (53) is constant and symmetric. Hence, considering (30) the vector of stress resultants follows from

$$\hat{\mathbf{S}} = \hat{\mathbf{D}}\,\hat{\mathbf{E}} \qquad\qquad \hat{\mathbf{E}} = \begin{bmatrix} \boldsymbol{\varepsilon} - \boldsymbol{\varepsilon}_0 \\ \boldsymbol{\kappa} - \boldsymbol{\kappa}_0 \\ \alpha \\ \alpha' \end{bmatrix}. \tag{54}$$

As can be seen torsion–bending coupling occurs if the reference point O and the shear center M with coordinates $\{m_2, m_3\}$ do not coincide. If the coordinates $\{\xi_2, \xi_3\}$ define principal axes of the cross–section and if $S = M = O$ all off–diagonal terms except $-G(I_0 - I_T)$ are zero. Furthermore, if the contribution of the bi–moment and of the bi–shear to the strain energy is neglectable a formulation with six stress resultants can be derived, see [17]. In this case one obtains the well–known elasticity matrix $\hat{\mathbf{D}} = \text{diag}\,[EA, GA, GA, GI_T, EI_{33}, EI_{22}]$.

5 FINITE ELEMENT FORMULATION

According to the isoparametric concept, the following kinematic variables are interpolated using standard Lagrangian shape functions $N_I(\xi)$ where $\xi \in [-1, +1]$. Within a typical element the position vector of the reference curve $\mathcal{S}_0^h$, the curve $\mathcal{S}^h$ of the current configuration and the parameter α are interpolated by

$$\mathbf{X}_0^h = \sum_{I=1}^{nel} N_I(\xi)\mathbf{X}_I\,, \qquad \mathbf{x}_0^h = \sum_{I=1}^{nel} N_I(\xi)(\mathbf{X}_I + \mathbf{u}_I)\,, \qquad \alpha^h = \sum_{I=1}^{nel} N_I(\xi)\alpha_I\,. \tag{55}$$

Here nel denotes the number of nodes at the element. For $nel \geq 3$ the reference curve of a space–curved beam is approximated by polynomial functions.
Furthermore the basis systems of the reference configuration and the current configuration are approximated using the same interpolation functions

$$\mathbf{A}_m^h = \sum_{I=1}^{nel} N_I(\xi)\,\mathbf{A}_{mI}\,, \qquad \mathbf{a}_m^h = \sum_{I=1}^{nel} N_I(\xi)\,\mathbf{a}_{mI}\,. \tag{56}$$

Thus the orthogonality condition of the basis systems $\mathbf{A}_m^h$ and $\mathbf{a}_m^h$ is only fulfilled at the nodes. Numerical investigations however show that no significant loss of accuracy follows from this approximation. The initial basis system $\mathbf{A}_{mI}$ is generated within the input of the finite element mesh whereas the current basis system at the finite element nodes is computed using the so–called Rodrigues formula

$$\mathbf{R}_I = \mathbf{a}_{mI} \otimes \mathbf{e}_m = \mathbf{1} + \frac{\sin\omega_I}{\omega_I}\boldsymbol{\Omega}_I + \frac{1-\cos\omega_I}{\omega_I^2}\boldsymbol{\Omega}_I^2 \tag{57}$$

with $\omega_I = |\boldsymbol{\omega}_I|$. Note, that formula (57) is singularity free for $0 \leq \omega_I < 2\pi$. The singularity at $n2\pi$ $(n = 1, 2, 3, ...)$ can be overcome by a multiplicative update of the rotation tensor after a certain number of load steps. The skew–symmetric tensor $\boldsymbol{\Omega}_I$ follows from the independent rotational parameters by $\boldsymbol{\Omega}_I = \text{skew}\,\boldsymbol{\omega}_I$. The basic equation reads $\boldsymbol{\Omega}_I\,\mathbf{h} = \boldsymbol{\omega}_I \times \mathbf{h}$ for all $\mathbf{h} \in \boldsymbol{R}^3$, thus the components are given by

$$\boldsymbol{\omega}_I = \begin{bmatrix} \omega_{1I} \\ \omega_{2I} \\ \omega_{3I} \end{bmatrix}, \qquad \boldsymbol{\Omega}_I = \begin{bmatrix} 0 & -\omega_{3I} & \omega_{2I} \\ \omega_{3I} & 0 & -\omega_{1I} \\ -\omega_{2I} & \omega_{1I} & 0 \end{bmatrix}. \tag{58}$$

The finite element approximations of the virtual displacements, basis vectors and the associated linearization are expressed as follows

$$\begin{aligned} \delta\mathbf{u}^h &= \sum_{I=1}^{nel} N_I(\xi)\delta\mathbf{u}_I\,, & \delta\alpha^h &= \sum_{I=1}^{nel} N_I(\xi)\delta\alpha_I\,, \\ \delta\mathbf{a}_m^h &= \sum_{I=1}^{nel} N_I(\xi)\delta\mathbf{a}_{mI}\,, & \Delta\delta\mathbf{a}_m^h &= \sum_{I=1}^{nel} N_I(\xi)\Delta\delta\mathbf{a}_{mI}\,. \end{aligned} \tag{59}$$

The derivative of the shape function $N_I(\xi)$ with respect to the arc–length S is obtained using the chain rule $N_I'(\xi) = N_I(\xi)_{,\xi} \, / |\mathbf{X}_{0,\xi}^h|$. Hence, the tangential vectors $\mathbf{X}_0'$ and $\mathbf{x}_0'$, the derivatives of the basis vectors $\mathbf{A}_m'$ and $\mathbf{a}_m'$ and associated variations and linearizations are given replacing N_I by N_I' in (55), (56) and (59).
The variation of the orthogonal basis system $\mathbf{a}_{mI}$ yields for all $\mathbf{h} \in \boldsymbol{R}^3$

$$\begin{aligned} \delta\mathbf{a}_{mI} &= \delta\mathbf{w}_I \times \mathbf{a}_{mI} = \mathbf{W}_{mI}^T \delta\mathbf{w}_I \,, \\ \mathbf{h} \cdot \delta\mathbf{a}_{mI} &= \mathbf{b}_{mI}(\mathbf{h}) \cdot \delta\mathbf{w}_I \,, \qquad \mathbf{b}_{mI}(\mathbf{h}) = \mathbf{a}_{mI} \times \mathbf{h} \end{aligned} \tag{60}$$

and

$$\mathbf{h} \cdot \delta\mathbf{a}_m = \sum_{I=1}^{nel} N_I \, \mathbf{b}_{mI}(\mathbf{h}) \cdot \delta\mathbf{w}_I \qquad\qquad \mathbf{h} \cdot \delta\mathbf{a}_m' = \sum_{I=1}^{nel} N_I' \, \mathbf{b}_{mI}(\mathbf{h}) \cdot \delta\mathbf{w}_I \,. \tag{61}$$

Thus, the virtual beam strains $\delta\hat{\mathbf{E}}$ considering (19) can be expressed as follows

$$\delta\hat{\mathbf{E}}^h = \sum_{I=1}^{nel} \mathbf{B}_I \, \delta\mathbf{v}_I \,, \qquad \mathbf{B}_I = \begin{bmatrix} N_I' \, \mathbf{R}^T & N_I \, \mathbf{B}_{\varepsilon I}^T & \mathbf{0} \\ \mathbf{0} & N_I' \, \mathbf{B}_{\kappa I}^T + N_I \, \mathbf{B}_{\kappa I}'^T & \mathbf{0} \\ \mathbf{0} & \mathbf{0} & N_I \\ \mathbf{0} & \mathbf{0} & N_I' \end{bmatrix} \tag{62}$$

with the virtual nodal displacement vector $\delta\mathbf{v}_I = [\delta\mathbf{u}_I, \delta\mathbf{w}_I, \delta\alpha_I]^T$ and

$$\begin{aligned} \mathbf{R} &:= [\mathbf{a}_1, \, \mathbf{a}_2, \, \mathbf{a}_3] & \mathbf{B}_{\varepsilon I} &:= [\mathbf{b}_{1I}(\mathbf{x}_0'), \, \mathbf{b}_{2I}(\mathbf{x}_0'), \, \mathbf{b}_{3I}(\mathbf{x}_0')] \\ \mathbf{B}_{\kappa I} &:= [\mathbf{b}_{2I}(\mathbf{a}_3), \, \mathbf{b}_{3I}(\mathbf{a}_1), \, \mathbf{b}_{1I}(\mathbf{a}_2)] & \mathbf{B}_{\kappa I}' &:= [\mathbf{b}_{3I}(\mathbf{a}_2'), \, \mathbf{b}_{1I}(\mathbf{a}_3'), \, \mathbf{b}_{2I}(\mathbf{a}_1')] \,. \end{aligned} \tag{63}$$

Next the finite element interpolation (55) – (63) is inserted into the linearized boundary value problem (27)

$$L[g(\mathbf{v}^h, \delta\mathbf{v}^h)] = \mathop{\mathsf{A}}_{e=1}^{numel} \sum_{I=1}^{nel} \sum_{K=1}^{nel} \delta\mathbf{v}_I^T \, (\mathbf{f}_I^e + \mathbf{K}_{IK}^e \Delta\mathbf{v}_K) \,. \tag{64}$$

Here, A denotes the standard assembly operator, *numel* the total number of elements to discretize the problem and $\Delta\mathbf{v}_K = [\Delta\mathbf{u}_K, \Delta\mathbf{w}_K, \Delta\alpha_K]^T$ the incremental displacement vector. Furthermore $\mathbf{f}_I^e$ and $\mathbf{K}_{IK}^e$ denote the sum of the internal and external nodal forces of node I and the tangential stiffness matrix of element e related to nodes I and K, respectively. Considering (62) one obtains

$$\mathbf{f}_I^e = \int_S (\mathbf{B}_I^T \hat{\mathbf{S}} - N_I \, \bar{\mathbf{q}}) \, \mathrm{d}S \,, \qquad \mathbf{K}_{IK}^e = \int_S (\mathbf{B}_I^T \, \hat{\mathbf{D}} \, \mathbf{B}_K + \mathbf{G}_{IK} + \mathbf{P}_{IK}) \, \mathrm{d}S \tag{65}$$

with

$$\begin{aligned} &\bar{\mathbf{q}} = [\bar{\mathbf{p}}, \, \bar{\mathbf{m}}_I, \, \bar{p}_{1I}]^T \\ &\bar{\mathbf{m}}_I = \mathbf{r}_I \times \bar{\mathbf{p}} \qquad \mathbf{r}_I = p_2 \, \mathbf{a}_{2I} + p_3 \, \mathbf{a}_{3I} + \alpha \, \bar{w}_p \, \mathbf{a}_{1I} \\ &\bar{p}_{1I} = \bar{w}_p \, \bar{\mathbf{p}} \cdot \mathbf{a}_{1I} \,. \end{aligned} \tag{66}$$

For linear elasticity the vector of stress resultants follows from the constitutive equation (54). For elastoplastic material behaviour $\hat{\mathbf{S}}$ and $\hat{\mathbf{D}}$ are obtained by numerical integration according to (22) and (30), respectively.

Next the geometric matrix $\mathbf{G}_{IK}$ is derived with the linearized virtual strains (29). For this purpose the second variation of the current basis system is derived as

$$\begin{aligned} \mathbf{h}\cdot\Delta\delta\mathbf{a}_{mI} &= \delta\mathbf{w}_I\cdot\mathbf{M}(\mathbf{a}_{mI},\mathbf{h})\Delta\mathbf{w}_I \\ \mathbf{M}(\mathbf{a}_{mI},\mathbf{h}) &= \frac{1}{2}(\mathbf{a}_{mI}\otimes\mathbf{h}+\mathbf{h}\otimes\mathbf{a}_{mI})+\frac{1}{2}(\mathbf{t}_{mI}\otimes\boldsymbol{\omega}_I+\boldsymbol{\omega}_I\otimes\mathbf{t}_{mI})+c_{10}\,\mathbf{1} \end{aligned} \tag{67}$$

where $\mathbf{t}_{mI}$ and c_{10} are specified in appendix A.3. This yields

$$\begin{aligned} \mathbf{h}\cdot\Delta\delta\mathbf{a}_{m} &= \sum_{I=1}^{nel} N_I\;\delta\mathbf{w}_I\cdot\mathbf{M}(\mathbf{a}_{mI},\mathbf{h})\,\Delta\mathbf{w}_I \\ \mathbf{h}\cdot\Delta\delta\mathbf{a}'_{m} &= \sum_{I=1}^{nel} N'_I\;\delta\mathbf{w}_I\cdot\mathbf{M}(\mathbf{a}_{mI},\mathbf{h})\,\Delta\mathbf{w}_I \end{aligned} \tag{68}$$

for all $\mathbf{h}\in\boldsymbol{R}^3$. As can be seen, the linearization of the basis system leads to a symmetric bi–linear form. One obtains

$$\mathbf{G}_{IK}=\begin{bmatrix} \mathbf{0} & N'_I N_K\,\mathbf{W}_{fK}^T & \mathbf{0} \\ N_I N'_K\,\mathbf{W}_{fI} & \mathbf{G}_{IK}^{ww} & \mathbf{0} \\ \mathbf{0} & \mathbf{0} & 0 \end{bmatrix}, \tag{69}$$

where

$$\begin{aligned} \mathbf{G}_{IK}^{ww} &= N'_I N_K\hat{\mathbf{W}}_{IK}^1+N_I N'_K\hat{\mathbf{W}}_{IK}^2+\delta_{IK}\left[\mathbf{M}(\mathbf{a}_{1I},\mathbf{h}_{1I})+\mathbf{M}(\mathbf{a}_{2I},\mathbf{h}_{2I})+\mathbf{M}(\mathbf{a}_{3I},\mathbf{h}_{3I})\right] \\ \mathbf{h}_{1I} &= N_I\,F^1\mathbf{x}'_0+N_I\,M^2\mathbf{a}'_3+N'_I\,M^3\mathbf{a}_2 \\ \mathbf{h}_{2I} &= N_I\,F^2\mathbf{x}'_0+N_I\,M^3\mathbf{a}'_1+N'_I\,M^1\mathbf{a}_3 \\ \mathbf{h}_{3I} &= N_I\,F^3\mathbf{x}'_0+N_I\,M^1\mathbf{a}'_2+N'_I\,M^2\mathbf{a}_1 \\ \hat{\mathbf{W}}_{IK}^1 &= M^1\mathbf{W}_{2I}\mathbf{W}_{3K}^T+M^2\mathbf{W}_{3I}\mathbf{W}_{1K}^T+M^3\mathbf{W}_{1I}\mathbf{W}_{2K}^T \\ \hat{\mathbf{W}}_{IK}^2 &= M^1\mathbf{W}_{3I}\mathbf{W}_{2K}^T+M^2\mathbf{W}_{1I}\mathbf{W}_{2K}^T+M^3\mathbf{W}_{2I}\mathbf{W}_{3K}^T \\ \mathbf{W}_{fI} &= \mathrm{skew}\left(F^1\mathbf{a}_{1I}+F^2\mathbf{a}_{2I}+F^3\mathbf{a}_{3I}\right). \end{aligned} \tag{70}$$

The external loading yields a contribution to the stiffness matrix if $\mathbf{r}_I\neq\mathbf{0}$. Considering (33) one obtains

$$\mathbf{P}_{IK}=-\begin{bmatrix} \mathbf{0} & \mathbf{0} & \mathbf{0} \\ \mathbf{0} & N_I\,\delta_{IK}\,\mathbf{M}(\mathbf{r}_I,\bar{\mathbf{p}}) & N_I N_K\,\bar{\mathbf{m}}_{1I} \\ \mathbf{0} & N_I N_K\,\bar{\mathbf{m}}_{1K}^T & 0 \end{bmatrix} \tag{71}$$

where $\bar{\mathbf{m}}_{1I}=\bar{w}_p\,\mathbf{a}_{1I}\times\bar{\mathbf{p}}$.
Application of the chain rule yields the differential arc–length $\mathrm{d}S=|\mathbf{X}_{0,\xi}^h|\,\mathrm{d}\xi$. The integration of the element residual and element stiffness matrix with respect to the coordinate S is performed numerically. To avoid shear locking uniform reduced integration is applied to all quantities. Finally the transformations of the axial vectors are introduced as follows

$$\delta\mathbf{w}_I=\mathbf{H}_I\,\delta\boldsymbol{\omega}_I \qquad\qquad \Delta\mathbf{w}_K=\mathbf{H}_K\,\Delta\boldsymbol{\omega}_K \tag{72}$$

where the tensor $\mathbf{H}$ is specified in appendix A.2. This leads to

$$\begin{aligned} L[g(\mathbf{v}^h,\delta\mathbf{v}^h)] &= \mathop{\mathbf{A}}_{e=1}^{numel}\sum_{I=1}^{nel}\sum_{K=1}^{nel}\delta\tilde{\mathbf{v}}_I^T\;(\tilde{\mathbf{f}}_I^e+\tilde{\mathbf{K}}_{IK}^e\Delta\tilde{\mathbf{v}}_K) \\ \delta\tilde{\mathbf{v}}_I &= [\delta\mathbf{u}_I,\delta\boldsymbol{\omega}_I,\delta\alpha_I]^T \qquad \Delta\tilde{\mathbf{v}}_K=[\Delta\mathbf{u}_K,\Delta\boldsymbol{\omega}_K,\Delta\alpha_K]^T \\ \tilde{\mathbf{f}}_I^e &= \mathbf{T}_I^T\mathbf{f}_I^e \qquad \tilde{\mathbf{K}}_{IK}^e=\mathbf{T}_I^T\mathbf{K}_{IK}^e\mathbf{T}_K \qquad \mathbf{T}_I=\mathrm{diag}[\mathbf{1},\,\mathbf{H}_I,\,1]\,. \end{aligned} \tag{73}$$

From eq. (73) one obtains a linear system of equations for the incremental nodal degrees of freedom. It is emphasized, that the update of the nodal displacements as well as of the rotational parameters is performed in an additive way. Thus, the equilibrium configuration is computed iteratively within the Newton iteration procedure.

Remark:
Within an alternative procedure one keeps $\Delta \mathbf{w}_I$ as unknown incremental rotational parameters. Thus the transformation (73) is not necessary anymore. However $\boldsymbol{\omega}_I$ must be known for the finite element interpolation (57) – (71). It can be obtained within the following simple update procedure

$$\begin{aligned} \boldsymbol{\omega}_K^{(n+1)} &= \boldsymbol{\omega}_K^{(n)} + \Delta\boldsymbol{\omega}_K \qquad \Delta\boldsymbol{\omega}_K = \mathbf{H}_K^{-1}\Delta\mathbf{w}_K \\ \mathbf{H}_K^{-1} &= \mathbf{1} - \tfrac{1}{2}\boldsymbol{\Omega}_K^{(n)} + \tfrac{1}{2}c_3\,\boldsymbol{\Omega}_K^{2(n)} \end{aligned} \tag{74}$$

where n denotes the index of the Newton iteration procedure. One can easily show that above expression fulfills $\mathbf{H}_K^{-1}\mathbf{H}_K = \mathbf{1}$. Again, the advantage of (74) compared with (73) is, that the transformation $\delta\mathbf{w}_I = \mathbf{H}_I\,\delta\boldsymbol{\omega}_I$ drops out. However, the algorithm (74) requires additional storage of the parameters $\boldsymbol{\omega}_K^{(n)}$.

6 NUMERICAL EXAMPLES

The element scheme has been implemented in an enhanced version of the program FEAP documented in Ref. [18]. In this section three examples with finite deformations and elastic–plastic material behaviour are presented. With the first example we investigate the stability behaviour of a beam assuming linear elastic material behaviour. The last two examples are concerned with the load carrying capacity of beam structures. The second example is a channel–section beam, where centroid, center of shear and loading point are not identical. With the last example we solve a coupled beam–shell problem. For comparison the investigated thin–walled beam structures are discretized using four–noded shell elements. These elements possess six nodal degrees of freedom which are identical to the first six degrees of freedom of the beam.

6.1 Lateral Torsional Buckling of a Single Span Girder

The first example is a single span girder with length $L = 150\,cm$ where an axial force F is applied at the centroid. Fig. 2 shows the cross–section of the channel section beam. The ratio of the width of the flange to the height of the web is relatively large. This type of cross–section is fairly sensitive against torsional buckling. The geometrical and material data are given in (75), where the moments of inertia are denoted according to the definitions in (51). The section quantities are determined with the finite element program as is described in [16].

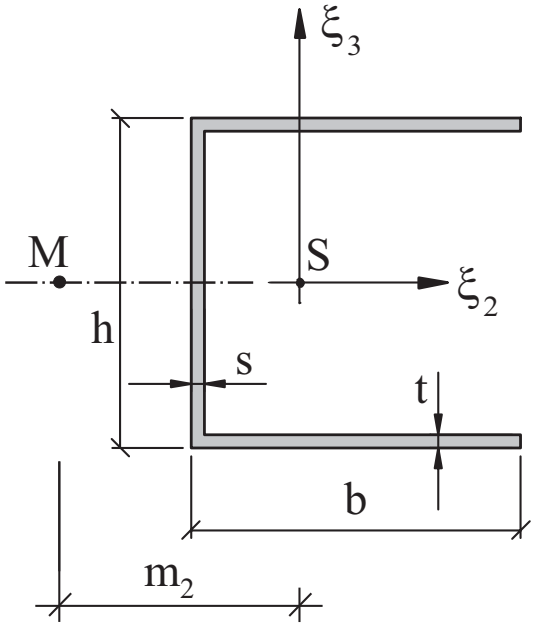

Figure 2: Cross–section of a single span girder

$$
\begin{array}{rcrl}
b &=& 10.0 & cm \\
h &=& 10.0 & cm \\
s &=& 0.2 & cm \\
t &=& 0.2 & cm \\
m_2 &=& 7.55 & cm
\end{array}
\qquad
\begin{array}{rcrl}
A &=& 5.92 & cm^2 \\
I_{33} &=& 110.8 & cm^4 \\
I_{22} &=& 64.49 & cm^4 \\
I_T &=& 0.0792 & cm^4 \\
I_{\tilde{w}} &=& 1108.2 & cm^6
\end{array}
\qquad (75)
$$

$$
\begin{array}{rcrl}
E &=& 21000 & kN/cm^2 \\
G &=& 8077 & kN/cm^2
\end{array}
$$

The boundary conditions are chosen as follows: The displacements at both supports except the axial displacement at the loaded cross–section are fixed. Furthermore the torsion angle is fixed at both ends. The other degrees of freedom are not restrained. The theoretical solution based on a second–order geometrical nonlinear Bernoulli beam theory including torsion–warping deformation may be found e.g. in Kollbrunner and Meister [19]. For this purpose we compute the following reference quantities with $n = 1$ for the lowest eigenvalue

$$
\begin{aligned}
F_1 &:= n^2 \frac{\pi^2 E I_{22}}{L^2} = 594.0\, kN \\
F_2 &:= n^2 \frac{\pi^2 E I_{33}}{L^2} = 1020.0\, kN \qquad (76) \\
F_3 &:= \frac{1}{i_M^2}(G I_T + n^2 \frac{\pi^2 E I_{\tilde{w}}}{L^2}) = 125.1\, kN\,.
\end{aligned}
$$

Here, $i_M^2 = i_P^2 + m_2^2$ follows with $i_P^2 = (I_{22} + I_{33})/A$. Furthermore F_1 describes the critical load for buckling in the symmetry plane. The theoretical critical load is given according to

$$
F_{cr} = 2 \left[\left(\frac{1}{F_2} + \frac{1}{F_3} \right) + \sqrt{\left(\frac{1}{F_2} - \frac{1}{F_3} \right)^2 + \frac{4}{F_2\, F_3} \left(\frac{m_2}{i_M} \right)^2} \right]^{-1} = 115.4\, kN\,. \qquad (77)
$$

As the result shows F_{cr} is close to the pure torsional buckling load F_3. Thus one obtains a significant reduction of the critical load perpendicular to the symmetry plane due to torsional buckling.
For the numerical solution we discretize the beam with $4, 8$ and 16 three–noded beam elements. The boundary conditions are set as described above. We solve the eigenvalue problem

$$(\mathbf{K}_T - \omega^2 \mathbf{1})\, \mathbf{\Phi} = \mathbf{0} \tag{78}$$

where the contribution of the element nodes to the tangential stiffness matrix $\mathbf{K}_T$ are given in (65). The critical loads F_{cr} are characterized by zero–eigenvalues ω_i with associated eigenvectors $\mathbf{\Phi}_i$. The minimum values for the different discretizations are given in table 1. As can be seen the agreement of our results with the solution of the second–order geometrical nonlinear Bernoulli theory is very good.

Table 1: Critical loads of the axially compressed single span girder

numel	F_{cr} in kN
4	115.3
8	115.0
16	115.0
analytical	115.4

6.2 Channel–section beam

A channel–section beam clamped at one end and subjected to a tip force at the free end is investigated next, see Fig. 3. We assume linear elastic and ideal plastic material behaviour with constants according to Fig. 3. The yield stress is $y_0 = 36\,kN/cm^2$. The developed beam model is compared with a shell model. The discretization is performed with 30 two–noded beam elements and in the second case with 360 four–noded shell elements. The shell discretization consists of 36 elements along the length direction, 6 elements along the web and 2 elements for each flange. In the following the vertical displacement w of point O at the cantilever tip is computed. For the elastic–plastic case we load up to a tip displacement $w = 250\,cm$ and then unload the structure.
The results for both models agree very good in the total range of the computed load deflection curve, see Fig. 4. This holds for elastic as well as for inelastic material behaviour. Fig. 5 shows a plot of the von Mises stresses according to eq. (38) for the ultimate state and the unloaded state. In Fig. 6 the stress distribution of the cross–section at a distance of 225 cm from the clamped end is given again for the ultimate state and the unloaded state. In the first case the cross–section is completely plastified, whereas in the second case residual stresses can be seen.

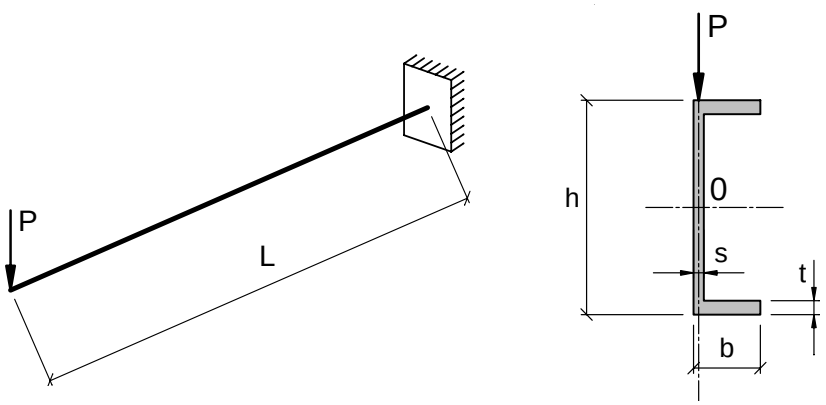

L	=	900	cm
h	=	30	cm
b	=	10	cm
s	=	1.0	cm
t	=	1.6	cm
E	=	21000	kN/cm^2
ν	=	0.30	

Figure 3: Channel–section beam with geometrical and material data

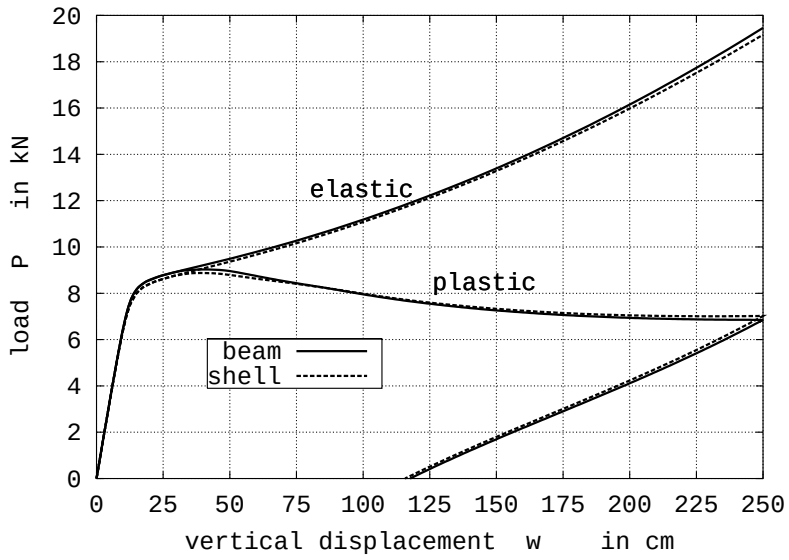

Figure 4: Load deflection curves of the channel–section beam

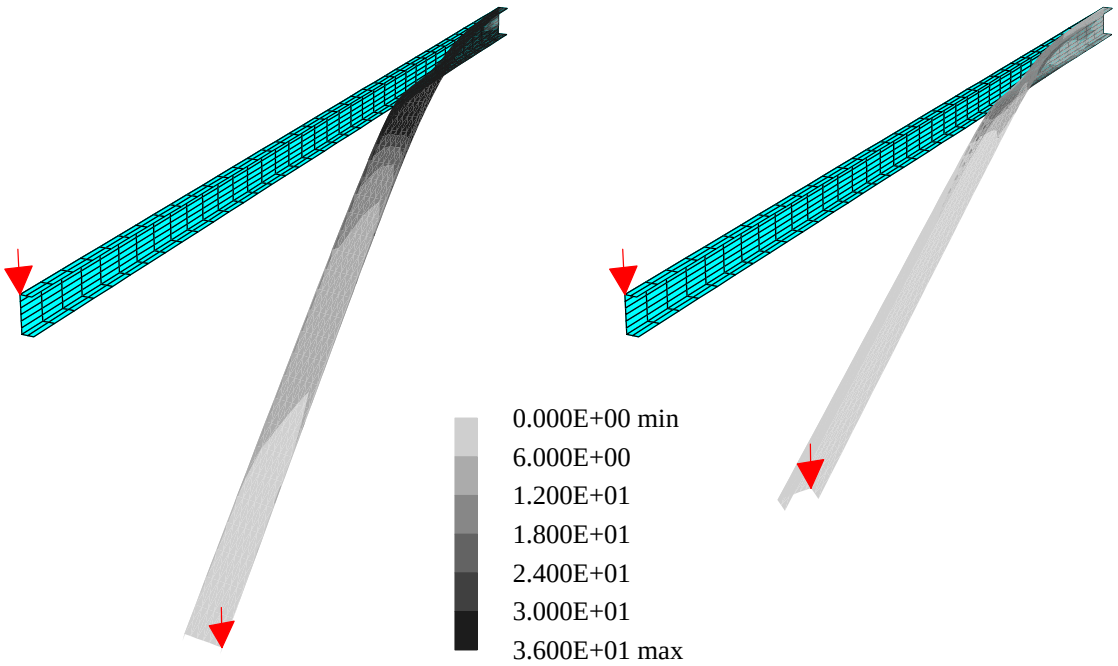

Figure 5: Von Mises stresses in kN/cm^2 for the ultimate state and unloaded state

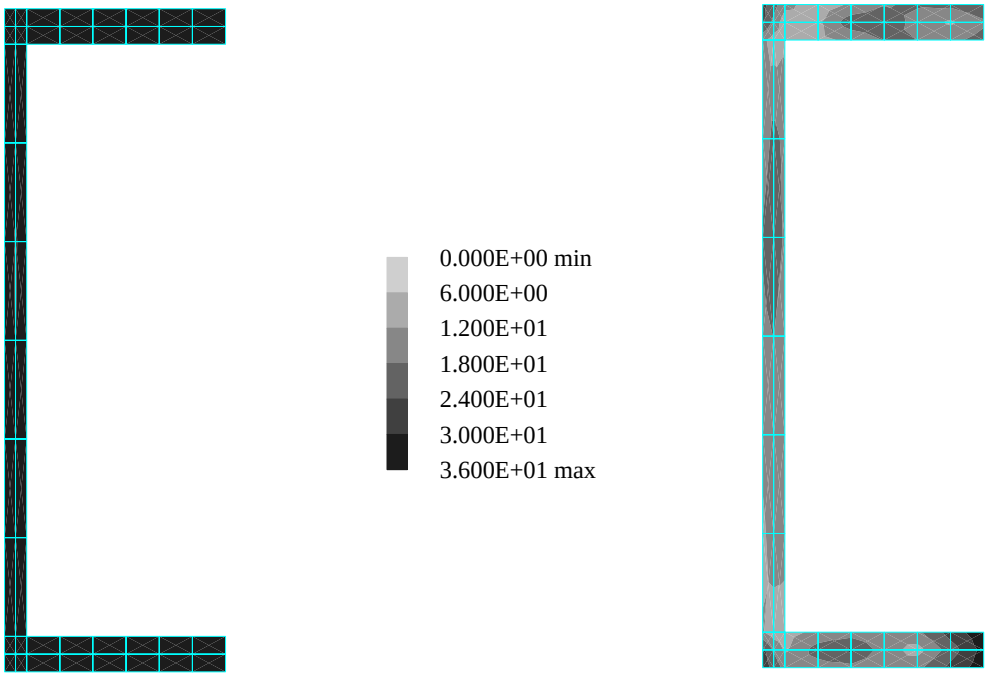

Figure 6: Von Mises stresses in kN/cm^2 of the cross–section at a distance of 225 cm from the clamped end for the ultimate state and unloaded state

6.3 Stiffened plate

With the last example coupling of the beam element with shell elements is investigated. Fig. 7 shows the cross–section of a rectangular plate of length ℓ and width b with an L–shaped stiffener. The structure is loaded by a single force, see Fig. 7. The geometrical and material data are given as follows

$$\begin{array}{rcrl} \ell &=& 300 & cm \\ b &=& 80 & cm \\ t &=& 0.5 & cm \end{array} \qquad \begin{array}{rcrl} E &=& 21000 & kN/cm^2 \\ \nu &=& 0.3 & \\ y_0 &=& 36 & kN/cm^2 \\ K &=& 0 & \end{array} \tag{79}$$

For comparison we apply two types of different discretizations. In both cases the plate is modeled using 20 four–noded shell elements in length direction and 10 elements in transverse direction. In the first case the L– shaped stiffener is discretized with 20 shell elements in length direction, 3 elements for the vertical leg and 2 elements for the horizontal leg. In the second case 20 two–noded beam elements are used. A computation without stiffener shows that the beam leads to a significant reduction of the deformation. The vertical displacement of the loading point is depicted in Fig. 8 for elastic and elastic–plastic material behaviour. Both models are in good agreement in large ranges of the computed load deflection curve. Plots of the von Mises stresses and of the equivalent plastic strains are depicted in Fig. 9, 10 and 11. The maximum plastic strain is about 5%. Fig. 11 shows that the structure undergoes large deformations.

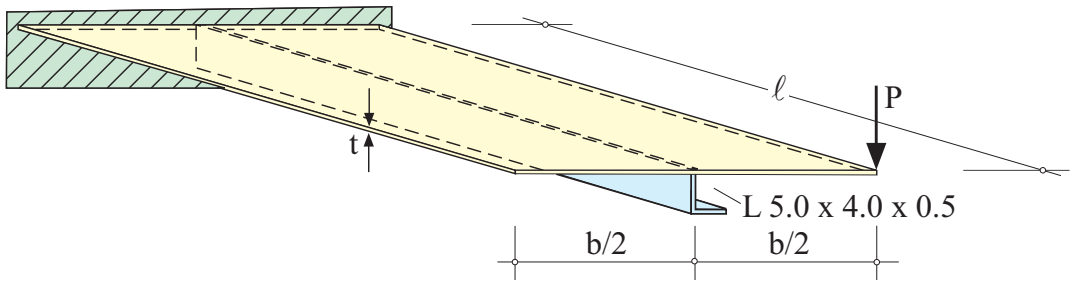

Figure 7: Clamped rectangular plate with stiffener

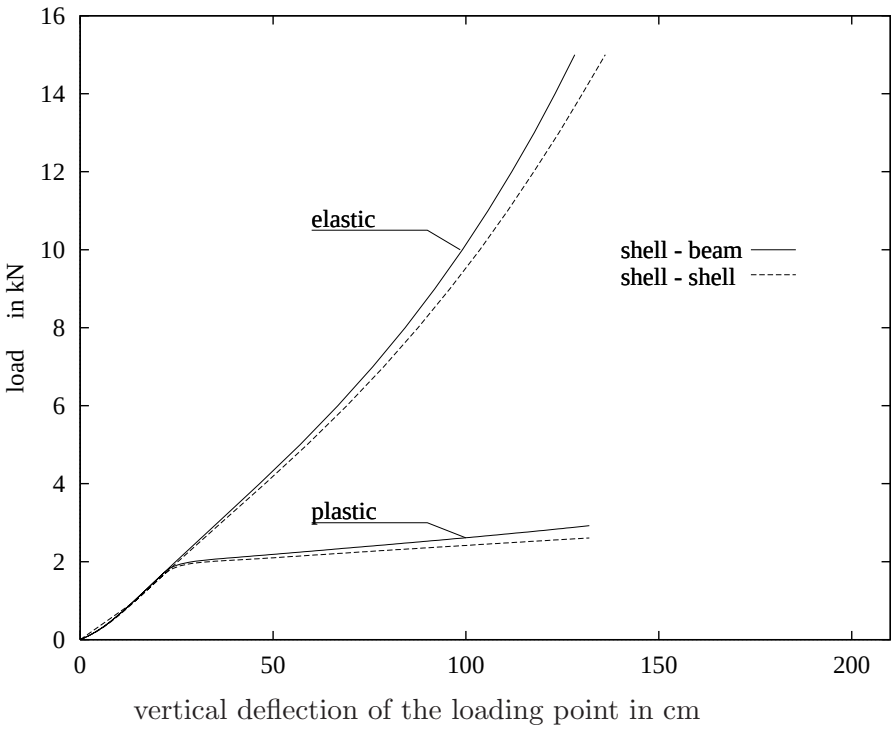

Figure 8: Load deflection curves of the stiffened plate

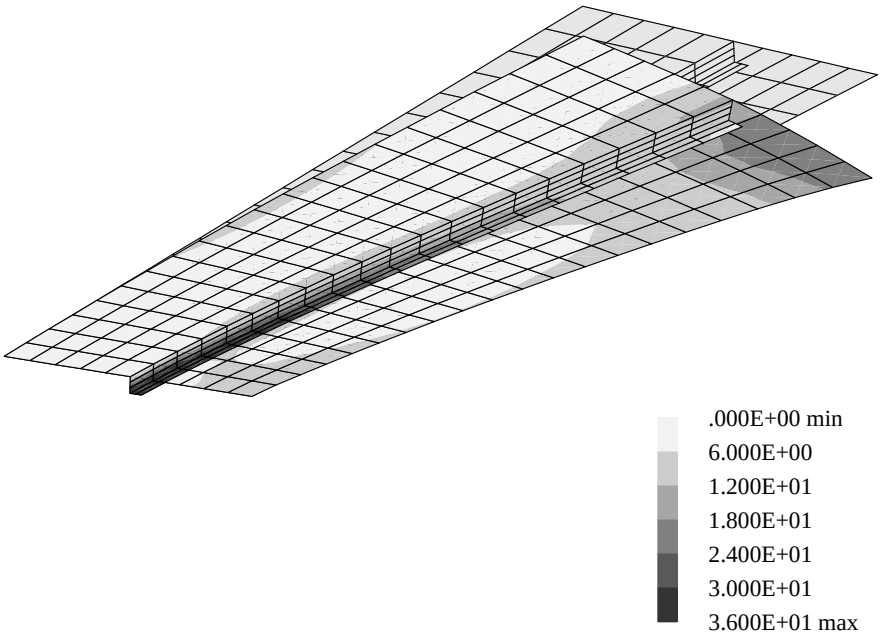

Figure 9: Von Mises stresses in kN/cm^2 for the stiffened plate at $w = 25\,cm$

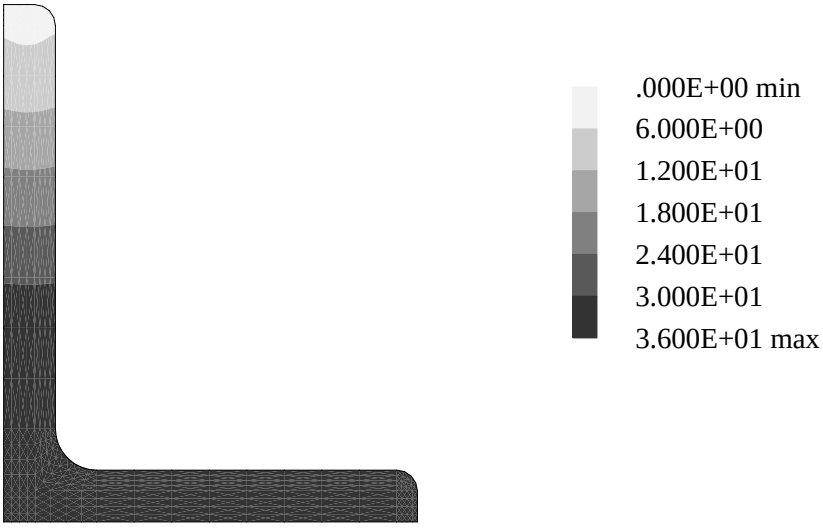

Figure 10: Von Mises stresses in kN/cm^2 for the stiffener at the clamped cross–section at $w = 25\,cm$

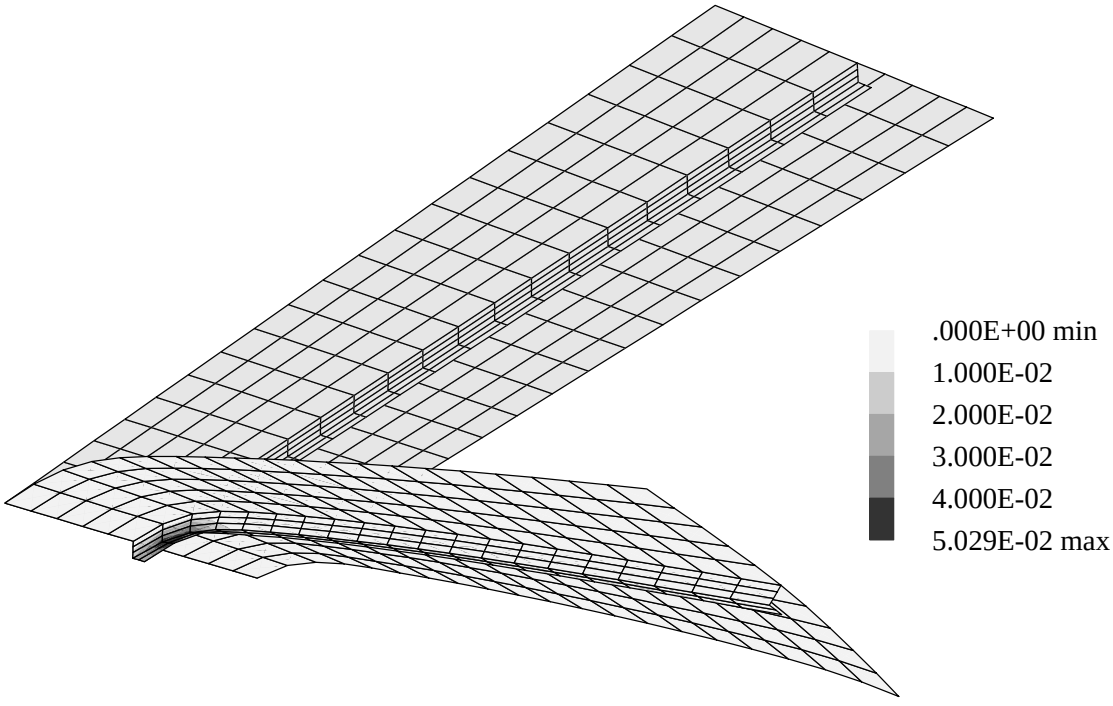

Figure 11: Equivalent plastic strains of the stiffened plate

7 CONCLUSIONS

In this paper a theory for three–dimensional beams with arbitrary cross–sections and an associated finite element formulation is developed. The beam strains are derived from the Green–Lagrangian strain tensor. Elastoplastic material behaviour applying the von Mises yield condition and associated flow rule is considered. Due to the nonlinear stress–strain relations the stress resultants and associated linearizations are obtained by numerical integration over the cross–sections. A finite beam element is developed using Lagrangian interpolation functions to approximate the kinematic quantities. Each node of the element possesses seven degrees of freedom. The basis systems at the nodes are evaluated using orthogonal transformations. Due to the chosen finite element approximation the linearization yields relative simple expressions for the symmetric tangent matrix. Examples show the applicability of the developed beam element applied to geometrical and physical nonlinear problems. Alternative discretizations of thin–walled cross–sections with shell elements show good agreement between the different models. Thus, the derived element can effectively be used to analyze the load–carrying capacities of spatial beam structures.

A APPENDIX

A.1 Proof of integrals (52)

Using $(3)_1$ the following integral is reformulated such that Green's formula can be applied. Hence inserting boundary condition $(3)_2$ yields

$$\begin{aligned}\int_A \bar{w}_{,2}\ \mathrm{d}A &= \int_A [(\xi_2\bar{w}_{,2}\,)_{,2}+(\xi_2\bar{w}_{,3}\,)_{,3}]\ \mathrm{d}A = \oint_C [\xi_2(\bar{w}_{,2}\,n_2+\bar{w}_{,3}\,n_3)]\ \mathrm{d}C \\ &= \oint_C [\xi_2(\xi_3 n_2-\xi_2 n_3)]\ \mathrm{d}C\,.\end{aligned} \tag{80}$$

Again application of Green's formula and considering $(51)_1$ leads to

$$\oint_C [\xi_2(\xi_3 n_2-\xi_2 n_3)]\ \mathrm{d}C = \int_A [(\xi_2\xi_3)_{,2}-\xi_{2,3}^2]\ \mathrm{d}A = \int_A \xi_3\ \mathrm{d}A = A\,s_3 \tag{81}$$

which proves $(52)_1$. Proceeding in an analogous way leads to $(52)_2$.

The following integral is reformulated in the same way as done above. Thus, we apply $(3)_1$, Green's formula and boundary condition $(3)_2$

$$\begin{aligned}\int_A (\bar{w}_{,2}^{\,2}+\bar{w}_{,3}^{\,2})\ \mathrm{d}A &= \int_A [(\bar{w}\,\bar{w}_{,2}\,)_{,2}+(\bar{w}\,\bar{w}_{,3}\,)_{,3}]\ \mathrm{d}A \\ &= \oint_C [\bar{w}(\bar{w}_{,2}\,n_2+\bar{w}_{,3}\,n_3)]\ \mathrm{d}C = \oint_C \bar{w}\,(\xi_3 n_2-\xi_2 n_3)\ \mathrm{d}C\,.\end{aligned} \tag{82}$$

Again application of Green's formula and considering the definition of Saint–Venant torsion modulus $(51)_4$ yields

$$\oint_C \bar{w}(\xi_3 n_2-\xi_2 n_3)\ \mathrm{d}C = \int_A (\bar{w}_{,2}\,\xi_3-\bar{w}_{,3}\,\xi_2)\ \mathrm{d}A = I_0 - I_T \tag{83}$$

which proves $(52)_3$.

Next using (4) and (5) we get

$$\int_A \bar{w}\xi_2\ \mathrm{d}A = \int_A (\bar{\xi}_2+s_2)(\tilde{w}-m_2\bar{\xi}_3+m_3\bar{\xi}_2)\ \mathrm{d}A = \bar{I}_{22}m_3-\bar{I}_{23}m_2 = I_{\bar{w}2} \tag{84}$$

which yields $(52)_4$. The expression for $I_{\bar{w}3}$ is obtained in an analogous way. Finally eq. $(52)_6$ can be derived considering the orthogonality conditions (4) and definition (5).

A.2 First Variation of the Orthogonal Basis System

The current orthogonal basis system can be written using the Rodrigues formula (57)

$$\mathbf{a}_i = \mathbf{R}\,\mathbf{e}_i \qquad \mathbf{R} = \mathbf{1} + \frac{\sin\omega}{\omega}\boldsymbol{\Omega} + \frac{1-\cos\omega}{\omega^2}\boldsymbol{\Omega}^2 \tag{85}$$

where $\omega = |\boldsymbol{\omega}|$ and $\boldsymbol{\Omega} = \operatorname{skew}\boldsymbol{\omega}$. To alleviate the notation the node index is omitted. The first variation, denoted here by the symbol δ, yields

$$\delta\mathbf{a}_i = \delta\mathbf{R}\mathbf{e}_i = \delta\mathbf{R}\mathbf{R}^T\mathbf{a}_i = \delta\mathbf{w}\times\mathbf{a}_i \tag{86}$$

with

$$\begin{aligned}\delta\mathbf{R} &= \frac{\sin\omega}{\omega}\delta\boldsymbol{\Omega} + \frac{1-\cos\omega}{\omega^2}(\delta\boldsymbol{\Omega}\boldsymbol{\Omega} + \boldsymbol{\Omega}\delta\boldsymbol{\Omega}) \\ &\quad + \left[\frac{\omega\cos\omega - \sin\omega}{\omega^2}\boldsymbol{\Omega} + \frac{\omega\,\sin\omega + 2\cos\omega - 2}{\omega^3}\boldsymbol{\Omega}^2\right]\delta\omega \\ \mathbf{R}^T &= \mathbf{1} - \frac{\sin\omega}{\omega}\boldsymbol{\Omega} + \frac{1-\cos\omega}{\omega^2}\boldsymbol{\Omega}^2\end{aligned} \tag{87}$$

with $\delta\omega = (\boldsymbol{\omega}\cdot\delta\boldsymbol{\omega})/\omega$. Inserting the identities

$$\boldsymbol{\Omega}^2 = \boldsymbol{\omega}\otimes\boldsymbol{\omega} - \omega^2\mathbf{1} \qquad \boldsymbol{\Omega}^3 = -\omega^2\boldsymbol{\Omega} \qquad \delta\boldsymbol{\Omega}\boldsymbol{\Omega} = \boldsymbol{\omega}\otimes\delta\boldsymbol{\omega} - (\boldsymbol{\omega}\cdot\delta\boldsymbol{\omega})\mathbf{1} \tag{88}$$

yields after some lengthy algebraic manipulation the skew–symmetric tensor

$$\begin{aligned}\delta\mathbf{R}\mathbf{R}^T &= (1 - c_2\omega^2)\delta\boldsymbol{\Omega} + c_1\,(\boldsymbol{\Omega}\delta\boldsymbol{\Omega} - \delta\boldsymbol{\Omega}\boldsymbol{\Omega}) + c_2\,(\boldsymbol{\omega}\cdot\delta\boldsymbol{\omega})\boldsymbol{\Omega} \\ c_1 &= \frac{1-\cos\omega}{\omega^2}\,, \qquad c_2 = \frac{\omega - \sin\omega}{\omega^3}\,.\end{aligned} \tag{89}$$

The associated axial vector reads

$$\delta\mathbf{w} = \mathbf{H}\,\delta\boldsymbol{\omega}\,, \qquad\qquad \mathbf{H} = \mathbf{1} + c_1\,\boldsymbol{\Omega} + c_2\,\boldsymbol{\Omega}^2\,. \tag{90}$$

A.3 Second Variation of the Orthogonal Basis System

The second variation of the orthogonal basis system is denoted by Δ. One obtains for all $\mathbf{h}\in\boldsymbol{R}^3$

$$\begin{aligned}\mathbf{h}\cdot\Delta\delta\mathbf{a}_i &= \mathbf{h}\cdot\Delta(\delta\mathbf{w}\times\mathbf{a}_i) \\ &= \mathbf{h}\cdot[\delta\mathbf{w}\times(\Delta\mathbf{w}\times\mathbf{a}_i) + \Delta\mathbf{H}\,\delta\boldsymbol{\omega}\times\mathbf{a}_i] \\ &= \delta\mathbf{w}\cdot[\mathbf{a}_i\otimes\mathbf{h} - (\mathbf{a}_i\cdot\mathbf{h})\mathbf{1}]\,\Delta\mathbf{w} + \mathbf{b}_i\cdot\Delta\mathbf{H}\,\delta\boldsymbol{\omega}\end{aligned} \tag{91}$$

where $\mathbf{b}_i = \mathbf{a}_i\times\mathbf{h}$. The second part in (91) yields with $\Delta\omega = (\boldsymbol{\omega}\cdot\Delta\boldsymbol{\omega})/\omega$

$$\begin{aligned}\mathbf{b}_i\cdot\Delta\mathbf{H}\,\delta\boldsymbol{\omega} &= \mathbf{b}_i\cdot[(\frac{\partial c_1}{\partial\omega}\boldsymbol{\Omega} + \frac{\partial c_2}{\partial\omega}\boldsymbol{\Omega}^2)\Delta\omega + c_1\Delta\boldsymbol{\Omega} + c_2(\Delta\boldsymbol{\Omega}\boldsymbol{\Omega} + \boldsymbol{\Omega}\Delta\boldsymbol{\Omega})]\,\delta\boldsymbol{\omega} \\ &= \delta\boldsymbol{\omega}\cdot\{[(-c_4\boldsymbol{\Omega} + c_5\boldsymbol{\Omega}^2)\mathbf{b}_i\otimes\boldsymbol{\omega}]\;\Delta\boldsymbol{\omega} + c_1\mathbf{b}_i\times\Delta\boldsymbol{\omega} + c_2(\Delta\boldsymbol{\Omega}\boldsymbol{\Omega} + \boldsymbol{\Omega}\Delta\boldsymbol{\Omega})\mathbf{b}_i\}\end{aligned} \tag{92}$$

with

$$\begin{aligned}c_3 &= \frac{\omega\sin\omega + 2\cos\omega - 2}{\omega^2(\cos\omega - 1)} \\ c_4 &= \frac{1}{\omega}\frac{\partial c_1}{\partial\omega} = -c_1\,c_3\,, \qquad c_5 = \frac{1}{\omega}\frac{\partial c_2}{\partial\omega} = c_6 - c_2\,c_3\,, \qquad c_6 = \frac{c_3 - c_2}{\omega^2}\,.\end{aligned} \tag{93}$$

Considering

$$\begin{aligned}\Delta\boldsymbol{\Omega}\boldsymbol{\Omega}\mathbf{b}_i &= (\mathbf{b}_i\times\boldsymbol{\omega})\times\Delta\boldsymbol{\omega} \\ \boldsymbol{\Omega}\Delta\boldsymbol{\Omega}\mathbf{b}_i &= [(\mathbf{b}_i\cdot\boldsymbol{\omega})\mathbf{1} - \mathbf{b}_i\otimes\boldsymbol{\omega}]\,\Delta\boldsymbol{\omega} \\ \mathbf{D}_i &:= c_1\mathbf{B}_i + c_2\mathbf{C}_i \\ \mathbf{B}_i &:= \mathbf{h}\otimes\mathbf{a}_i - \mathbf{a}_i\otimes\mathbf{h} \\ \mathbf{C}_i &:= \boldsymbol{\omega}\otimes\mathbf{b}_i - \mathbf{b}_i\otimes\boldsymbol{\omega} \\ \mathbf{s}_i &:= (-c_2\,\mathbf{1} - c_4\,\boldsymbol{\Omega} + c_5\,\boldsymbol{\Omega}^2)\,\mathbf{b}_i\end{aligned} \tag{94}$$

we get

$$\mathbf{b}_i \cdot \Delta\mathbf{H}\,\delta\boldsymbol{\omega} = \delta\boldsymbol{\omega} \cdot [\mathbf{s}_i \otimes \boldsymbol{\omega} + \mathbf{D}_i + c_2(\mathbf{b}_i \cdot \boldsymbol{\omega})\mathbf{1}]\,\Delta\boldsymbol{\omega}\,. \tag{95}$$

Inserting this result into (91) yields

$$\begin{aligned} \mathbf{h} \cdot \Delta\delta\mathbf{a}_i &= \delta\mathbf{w} \cdot \mathbf{M}_i\,\Delta\mathbf{w} \\ \mathbf{M}_i &= \mathbf{a}_i \otimes \mathbf{h} - (\mathbf{a}_i \cdot \mathbf{h})\mathbf{1} + \mathbf{H}^{T-1}\,[\mathbf{s}_i \otimes \boldsymbol{\omega} + \mathbf{D}_i + c_2(\mathbf{b}_i \cdot \boldsymbol{\omega})\mathbf{1}]\,\mathbf{H}^{-1}\,. \end{aligned} \tag{96}$$

Within a multiplicative update procedure as is applied in [7] or [8] the last term in (96) is missing and one obtains a non–symmetric tangent operator. It follows if $\delta\mathbf{w} = \delta\boldsymbol{\omega}$ is chosen, thus $\mathbf{H} = \mathbf{1}$. However, this is justified for a multiplicative procedure with unknown rotation increments $\Delta\boldsymbol{\omega}$ since $\mathbf{H}(\Delta\boldsymbol{\omega})$ approaches the unit tensor at an equilibrium configuration.
The symmetry of $\mathbf{M}_i$ is shown in the following. For this purpose $\mathbf{M}_i$ is split in a symmetric and a skew–symmetric part, thus $\mathbf{M}_i = \mathbf{M}_i^S + \mathbf{M}_i^A$ where we show that the skew–symmetric part cancels out. We introduce

$$\begin{aligned} \mathbf{w}_i := \mathbf{H}^{T-1}\mathbf{s}_i &= -c_3\mathbf{b}_i + c_6\,(\mathbf{b}_i \cdot \boldsymbol{\omega})\,\boldsymbol{\omega} \\ \mathbf{H}^{T-1}\,\boldsymbol{\omega} &= \boldsymbol{\omega} \end{aligned} \tag{97}$$

where the first eq. follows immediately by multiplying $(97)_1$ with $\mathbf{H}^T$, comparing the coefficients and considering (93). The second equation is evident with (74) and $\boldsymbol{\Omega}\,\boldsymbol{\omega} = \mathbf{0}$. One obtains

$$\begin{aligned} \mathbf{M}_i^A &= \frac{1}{2}\,(\mathbf{M}_i - \mathbf{M}_i^T) \\ &= \frac{1}{2}(\mathbf{a}_i \otimes \mathbf{h} - \mathbf{h} \otimes \mathbf{a}_i) - \frac{1}{2}c_3(\mathbf{b}_i \otimes \boldsymbol{\omega} - \boldsymbol{\omega} \otimes \mathbf{b}_i) + \mathbf{H}^{T-1}\,\mathbf{D}_i\,\mathbf{H}^{-1} \\ &= -\frac{1}{2}\mathbf{B}_i + \frac{1}{2}c_3\mathbf{C}_i + \mathbf{H}^{T-1}\,\mathbf{D}_i\,\mathbf{H}^{-1}\,. \end{aligned} \tag{98}$$

Considering (74) we get

$$\begin{aligned} \mathbf{H}^{T-1}\,\mathbf{D}_i\,\mathbf{H}^{-1} &= \mathbf{D}_i + \tfrac{1}{2}(\boldsymbol{\Omega}\mathbf{D}_i - \mathbf{D}_i\boldsymbol{\Omega}) + \tfrac{1}{2}c_3(\boldsymbol{\Omega}^2\mathbf{D}_i + \mathbf{D}_i\boldsymbol{\Omega}^2) \\ &\quad + \tfrac{1}{4}c_3(\boldsymbol{\Omega}\mathbf{D}_i\boldsymbol{\Omega}^2 - \boldsymbol{\Omega}^2\mathbf{D}_i\boldsymbol{\Omega}) - \tfrac{1}{4}\boldsymbol{\Omega}\mathbf{D}_i\boldsymbol{\Omega} + \tfrac{1}{4}c_3^2\boldsymbol{\Omega}^2\mathbf{D}_i\boldsymbol{\Omega}^2 \end{aligned} \tag{99}$$

with

$$\begin{aligned} \mathbf{D}_i\boldsymbol{\Omega} &= \boldsymbol{\omega} \otimes \mathbf{d}_i - (\mathbf{d}_i \cdot \boldsymbol{\omega})\mathbf{1} \\ \boldsymbol{\Omega}\mathbf{D}_i\boldsymbol{\Omega} &= -(\mathbf{d}_i \cdot \boldsymbol{\omega})\,\boldsymbol{\Omega} \\ \boldsymbol{\Omega}\mathbf{D}_i\boldsymbol{\Omega}^2 &= \boldsymbol{\Omega}^2\mathbf{D}_i\boldsymbol{\Omega} = -(\mathbf{d}_i \cdot \boldsymbol{\omega})\,\boldsymbol{\Omega}^2 \\ \boldsymbol{\Omega}^2\mathbf{D}_i + \mathbf{D}_i\boldsymbol{\Omega}^2 &= -(\mathbf{d}_i \cdot \boldsymbol{\omega})\boldsymbol{\Omega} - \omega^2\mathbf{D}_i \\ \boldsymbol{\Omega}^2\mathbf{D}_i\boldsymbol{\Omega}^2 &= \omega^2(\mathbf{d}_i \cdot \boldsymbol{\omega})\,\boldsymbol{\Omega} \end{aligned} \tag{100}$$

thus

$$\begin{aligned} &\mathbf{H}^{T-1}\,\mathbf{D}_i\,\mathbf{H}^{-1} = c_7\,\mathbf{D}_i + \tfrac{1}{2}(\boldsymbol{\Omega}\mathbf{D}_i - \mathbf{D}_i\boldsymbol{\Omega}) + c_8(\mathbf{d}_i \cdot \boldsymbol{\omega})\,\boldsymbol{\Omega} \\ &c_7 = 1 - \tfrac{1}{2}c_3\omega^2 \qquad c_8 = \tfrac{1}{4} - \tfrac{1}{2}c_3 + \tfrac{1}{4}c_3^2\omega^2 \end{aligned} \tag{101}$$

with $\mathbf{d}_i = c_1\,\mathbf{b}_i + c_2\,\mathbf{b}_i \times \boldsymbol{\omega}$.
Using $\mathbf{d}_i \cdot \boldsymbol{\omega} = c_1\mathbf{b}_i \cdot \boldsymbol{\omega}$, $(94)_3$ and

$$\frac{1}{2}(\boldsymbol{\Omega}\mathbf{D}_i - \mathbf{D}_i\boldsymbol{\Omega}) = -\frac{1}{2}c_2(\mathbf{b}_i \cdot \boldsymbol{\omega})\,\boldsymbol{\Omega} + \frac{1}{2}c_2\omega^2\,\mathbf{B}_i - \frac{1}{2}c_1\,\mathbf{C}_i \tag{102}$$

one obtains the final version of the skew–symmetric part as

$$\mathbf{M}_i^A = (c_1 c_8 - \frac{1}{2} c_2)\,(\mathbf{b}_i \cdot \boldsymbol{\omega})\,\boldsymbol{\Omega} + (-\frac{1}{2} + c_1 c_7 + \frac{1}{2} c_2 \omega^2)\,\mathbf{B}_i + (\frac{1}{2} c_3 + c_2 c_7 - \frac{1}{2} c_1)\,\mathbf{C}_i\,, \quad (103)$$

where one can easily show that the coefficients vanish, and thus $\mathbf{M}_i^A \equiv \mathbf{0}$.
The symmetric part of $\mathbf{M}_i$ reads

$$\begin{aligned} \mathbf{M}_i^S &= \tfrac{1}{2}\,(\mathbf{M}_i + \mathbf{M}_i^T) \\ &= \tfrac{1}{2}(\mathbf{a}_i \otimes \mathbf{h} + \mathbf{h} \otimes \mathbf{a}_i) - (\mathbf{a}_i \cdot \mathbf{h})\mathbf{1} + \tfrac{1}{2}(\mathbf{w}_i \otimes \boldsymbol{\omega} + \boldsymbol{\omega} \otimes \mathbf{w}_i) + c_2(\mathbf{b}_i \cdot \boldsymbol{\omega})\,\mathbf{H}^{T-1}\,\mathbf{H}^{-1} \end{aligned} \quad (104)$$

and with $\mathbf{H}^{-1}$ according to (74) and (88)

$$\mathbf{H}^{T-1}\mathbf{H}^{-1} = \mathbf{1} + c_9 \boldsymbol{\Omega}^2 \qquad c_9 = -\frac{1}{4} + c_3 - \frac{1}{4}\omega^2 c_3^2 \quad (105)$$

we may express (104) as follows

$$\begin{aligned} \mathbf{M}_i^S &= \tfrac{1}{2}(\mathbf{a}_i \otimes \mathbf{h} + \mathbf{h} \otimes \mathbf{a}_i) + \tfrac{1}{2}(\mathbf{t}_i \otimes \boldsymbol{\omega} + \boldsymbol{\omega} \otimes \mathbf{t}_i) + c_{10}\mathbf{1} \\ \mathbf{t}_i &= -c_3\,\mathbf{b}_i + (c_6 + c_2 c_9)\,(\mathbf{b}_i \cdot \boldsymbol{\omega})\,\boldsymbol{\omega} \\ c_{10} &= c_2(1 - c_9\,\omega^2)\,(\mathbf{b}_i \cdot \boldsymbol{\omega}) - (\mathbf{a}_i \cdot \mathbf{h})\,. \end{aligned} \quad (106)$$

Applying a multiplicative update procedure the rotational parameters $\boldsymbol{\omega}$ are replaced by $\Delta\boldsymbol{\omega}$ which vanish in the Newton iteration process. Thus all terms in $\boldsymbol{\omega}$ in eq. (106) cancel out. This again shows that $\mathbf{M}$ becomes symmetric at an equilibrium configuration within the multiplicative procedure [7].

References

1. J.H. Argyris, O. Hilpert, G.A. Malejannakis and D.W. Scharpf, On the geometrical stiffness of a beam in space– A consistent v.w. approach, Comp. Meth. Appl. Mech. Engrg. 20 (1979) 105–131. 1

2. K.J. Bathe and S. Bolourchi, Large displacement analysis of three–dimensional beam structures, Int. J. Num. Meth. Engng. 14 (1979) 961–986. 1

3. T. Belytschko and B.J. Hsieh, Non–linear finite element analysis with convected co-ordinates, Int. J. Num. Meth. Engng. 7 (1973) 255–271. 1

4. M.A. Crisfield, A consistent co–rotational formulation for non–linear three–dimensional beam elements, Comp. Meth. Appl. Mech. Engrg. 81 (1990) 131–150. 1

5. B. Nour–Omid and C.C. Rankin, Finite rotation analysis and consistent linearization using projectors, Comp. Meth. Appl. Mech. Engrg. 93 (1991) 353–384. 1

6. E. Reissner, On finite deformations of space–curved beams, J. Appl. Math. Phys. (ZAMP) 32 (1981) 734–744. 1

7. J.C. Simo and L. Vu–Quoc, A three–dimensional finite–strain rod model. Part II: Computational aspects, Comp. Meth. Appl. Mech. Engrg. 58(1) (1986) 79–116. 1, A.3, A.3

8. J.C. Simo and L. Vu–Quoc, A geometrically–exact rod model incorporating shear and torsion–warping deformation, Int. J. Solids Structures 27(3) (1991) 371–393. 1, A.3

9. A. Cardona and M. Géradin, A beam finite element non–linear theory with finite rotations, Int. J. Num. Meth. Engng. 26 (1988) 2403–2438. 1

10. A. Ibrahimbegović, Computational aspects of vector–like parametrization of three–dimensional finite rotations, Int. J. Num. Meth. Engng. 38 (1995) 3653–3673. 1

11. E. Reissner, Some considerations on the problem of torsion and flexure of prismatical beams, Int. J. Solids Structures 15 (1979) 41–53. 1

12. E. Reissner, On a simple variational analysis of small finite deformations of prismatical beams, J. Appl. Math. Phys. (ZAMP) 34 (1983) 642–648. 1, 3.2

13. M. Géradin and D. Rixen, Parametrization of finite rotations in computational dynamics: a review, Revue européenne des éléments finis, 4 (1995) 497–553 2

14. P. Betsch, A. Menzel, E. Stein, On the parametrization of finite rotations in computational mechanics A classification of concepts with application to smooth shells, Comp. Meth. Appl. Mech. Engrg. 155 (1998) 273–305. 2

15. S.P. Timoshenko and J.N. Goodier, Theory of Elasticity, 3rd edition, McGraw–Hill International Book Company, 1984. 2

16. F. Gruttmann, W. Wagner and R. Sauer, Zur Berechnung von Wölbfunktion und Torsionskennwerten beliebiger Stabquerschnitte mit der Methode der finiten Elemente, Bauingenieur 73(3) (1998) 138–143. 3.3, 4.2, 6.1

17. F. Gruttmann, R. Sauer and W. Wagner W, A geometrical nonlinear eccentric 3D–beam element with arbitrary cross–sections, Comp. Meth. Appl. Mech. Engrg. 160 (1998) 383–400. 3.1, 4.2

18. O.C. Zienkiewicz and R.L. Taylor, The Finite Element Method, 4th edition, Volume 1 (McGraw Hill, London, 1988). 6

19. C.F. Kollbrunner and M. Meister, Knicken, Biegedrillknicken, Kippen : Theorie und Berechnung von Knickstäben; Knickvorschriften, 2nd edition (Springer, Berlin, 1961). 6.1